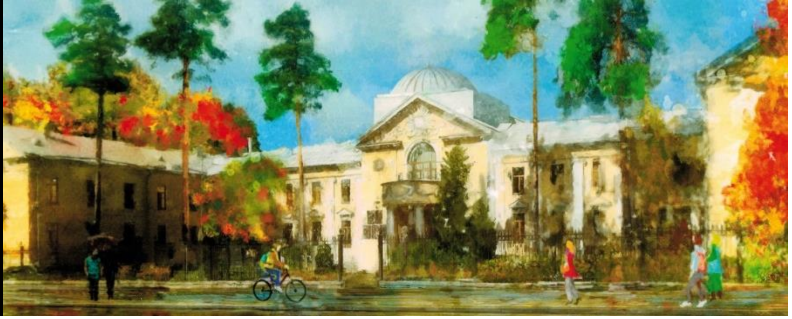

Outflows from the type I quasar at high-z: molecular gas in the host galax~~ie~~s y

P. Noterdaeme[2], **S.A. Balashev[1]**,

and J.K. Krogager, F. Combes, N. Gupta, R. Srianand, P. Laursen, P. Petitjean, J.P.U. Fynbo, …

[1]Ioffe Institute, Saint-Petersburg, Russia
[2]Institut d'Astrophysique de Paris, France

14 April 2021

Quasars

Quasars are active galactic nuclei at high redshifts

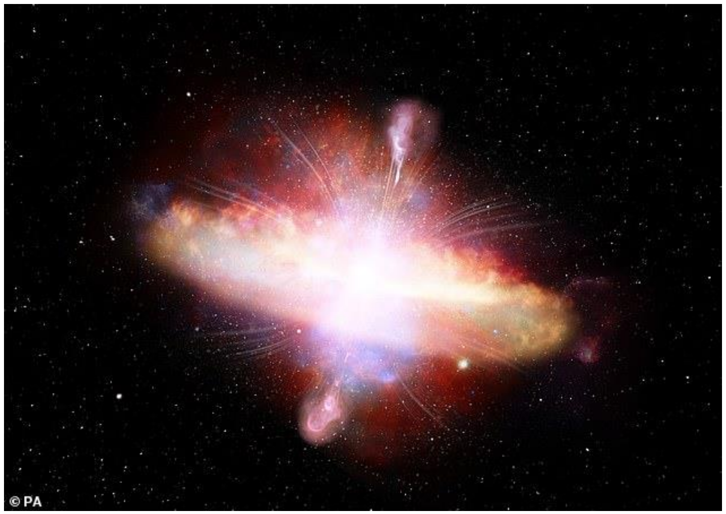

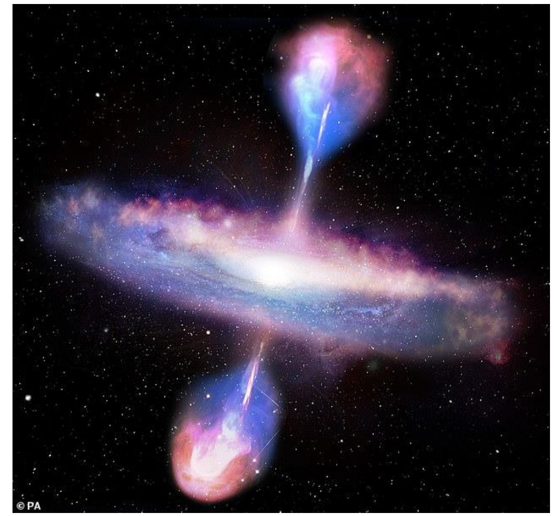

Feedback from active galactic nuclei (AGN) is an essential element in modern models of galaxy formation and evolution (e.g. Silk & Rees 1998). It may **quench star formation** (e.g. Pontzen et al. 2017), **impact galaxy morphology** (Dubois et al. 2016), regulate the growth of the super-massive black hole (Volonteri et al. 2016)

Quasars

In scheme for galaxy evolution, QSO are the particular stage

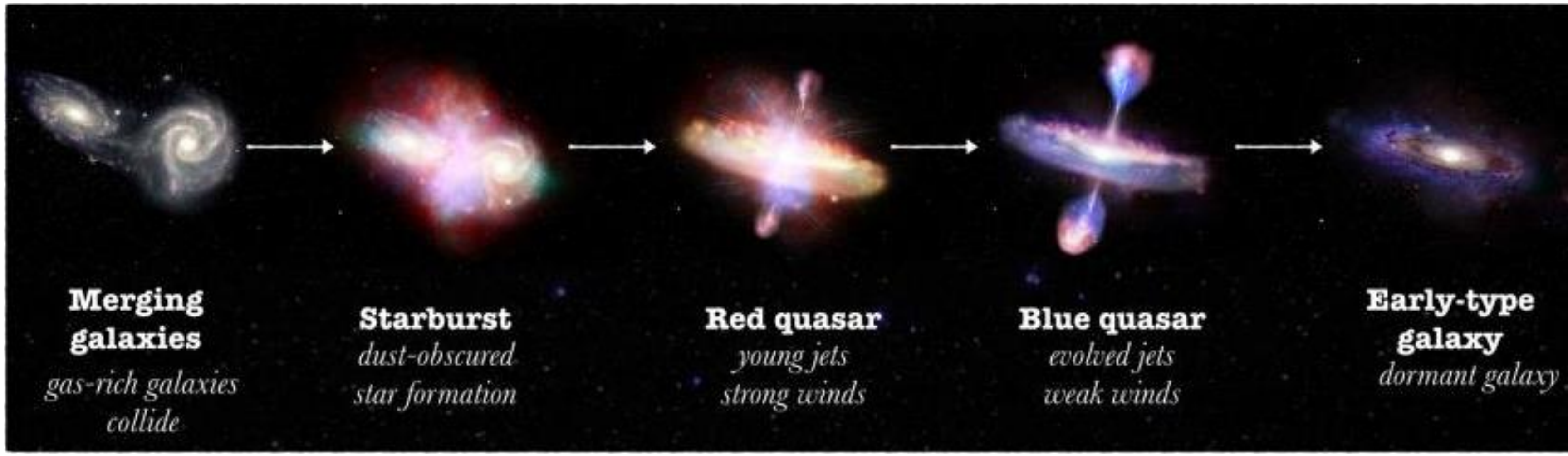

…with two observed classes (**obscured** – red and **unobscured** – blue) following each others.

The conversion of obscured to unobscured phase is though to be due to (or associated with) powerful outflows.

Quasar (AGN) outflows

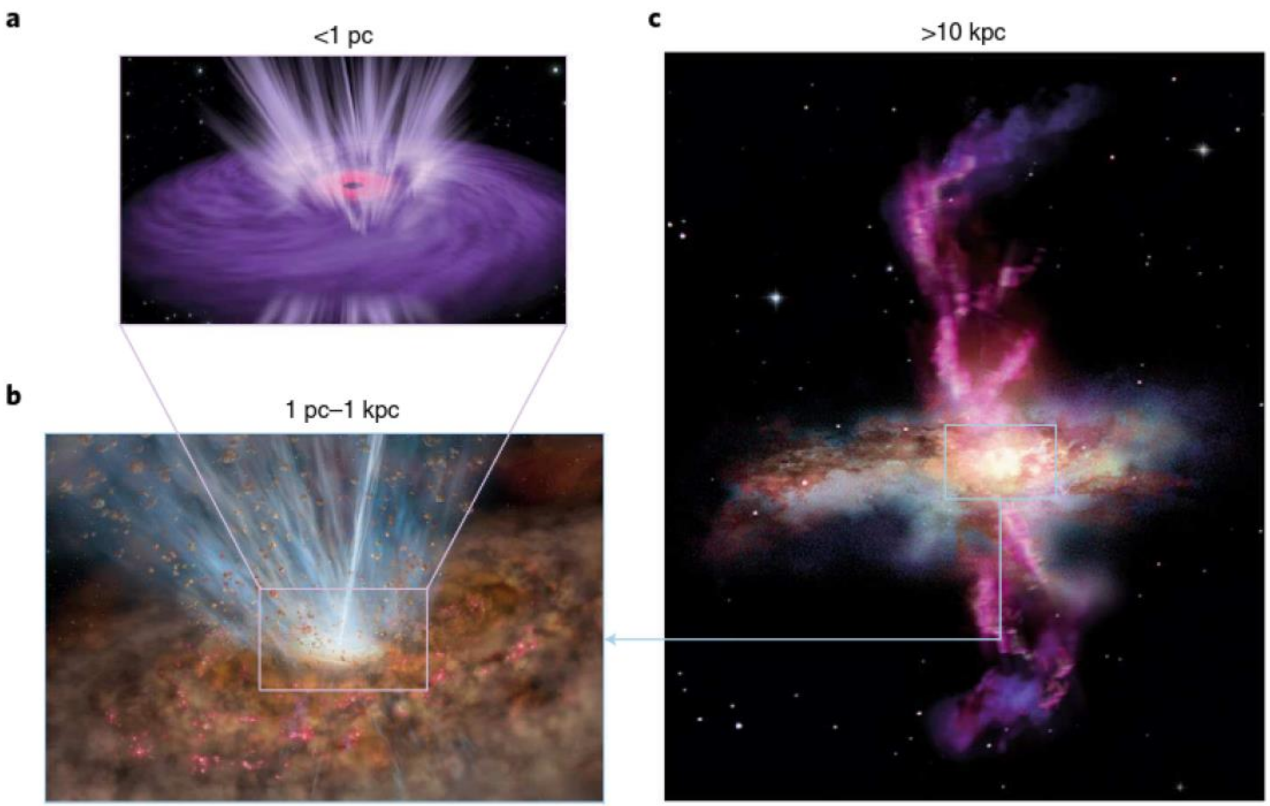

Cicone et al. (2018)

Many:

- Scales
- Phases
- Probes
- Difficulties

Outflow gas phase	Primary tracers	Average gas temperature, $<T_{gas}>$ (K)	Average gas density, $<n_{gas}>$ (particles per cm^3)
Highly ionized	X-ray absorption lines	10^6–10^7	10^6–10^8
Ionized	[O III]; Hα	10^3–10^4	10^2–10^4
Neutral atomic	H I 21cm; NaID; [C II]	10^2–10^3	1-10^2
Molecular	CO; OH; [C II]; H_2 infrared lines	10-10^2	$\geq 10^3$

+ H_2 in UV lines (this talk)

Quasar (AGN) outflows

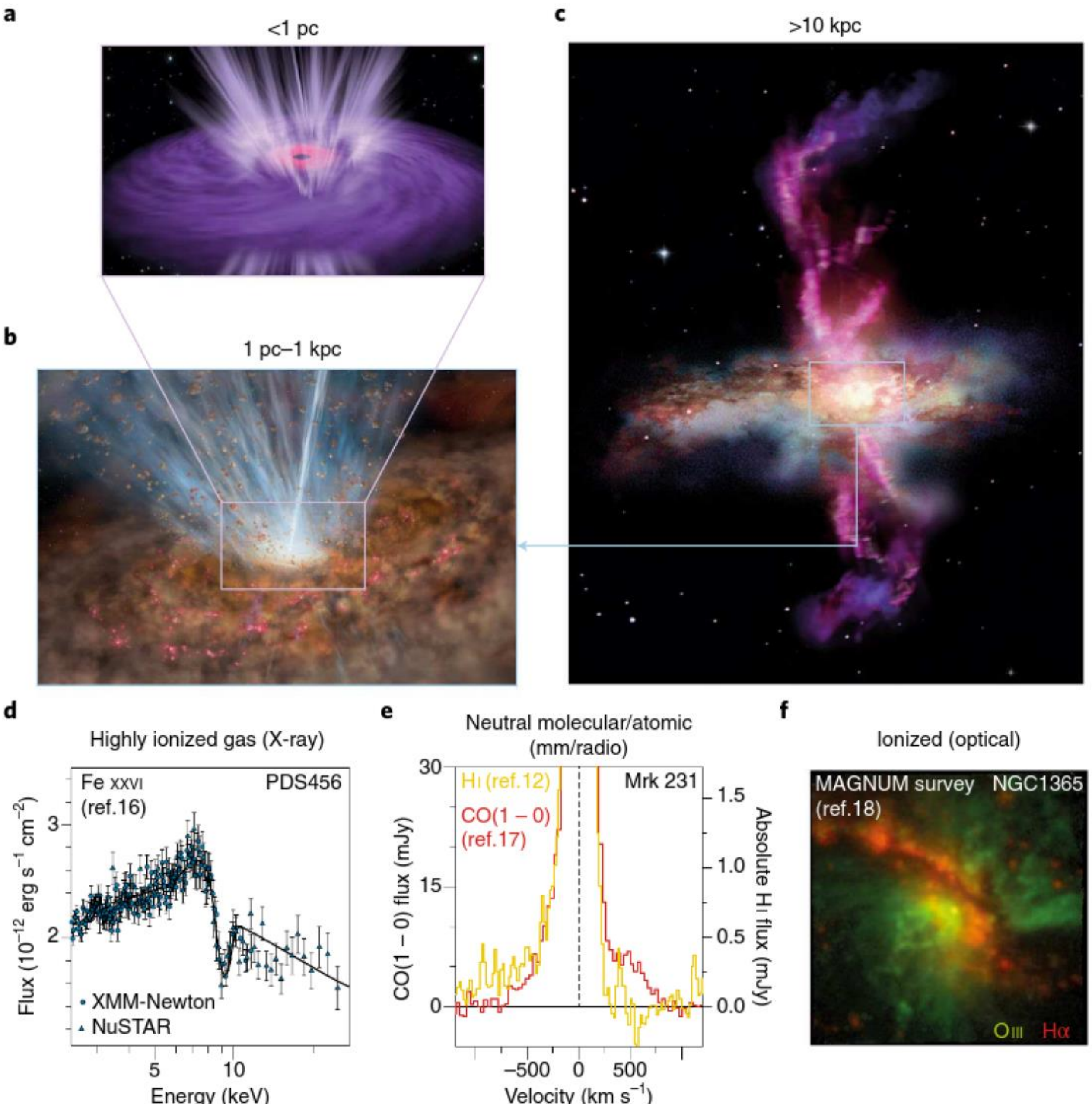

Cicone et al. (2018)

Many:

- Scales
- Phases
- Probes
- Difficulties

Quasar (AGN) outflows

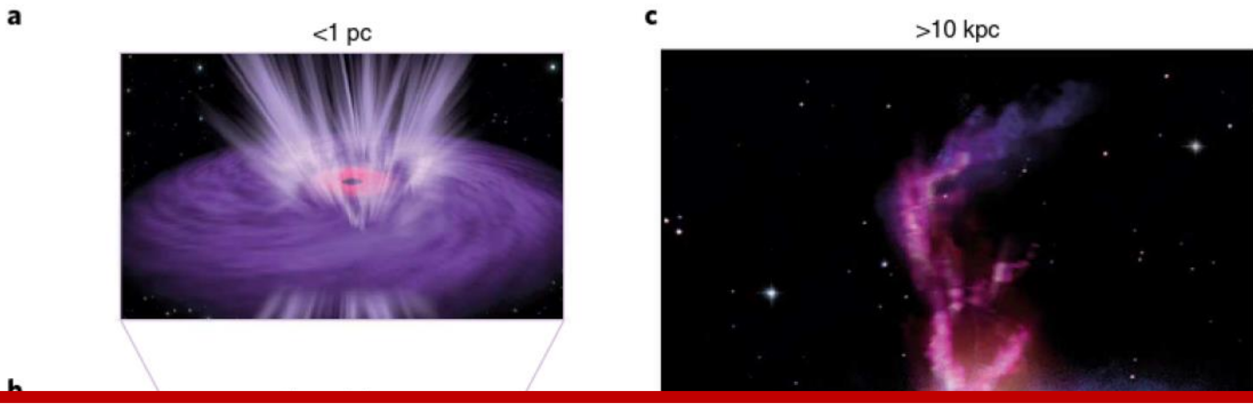

Cicone et al. (2018)

At high redshifts (z>1) there is an epoch of quasar activity,

However, the spatial resolution is very limited > a few kpc

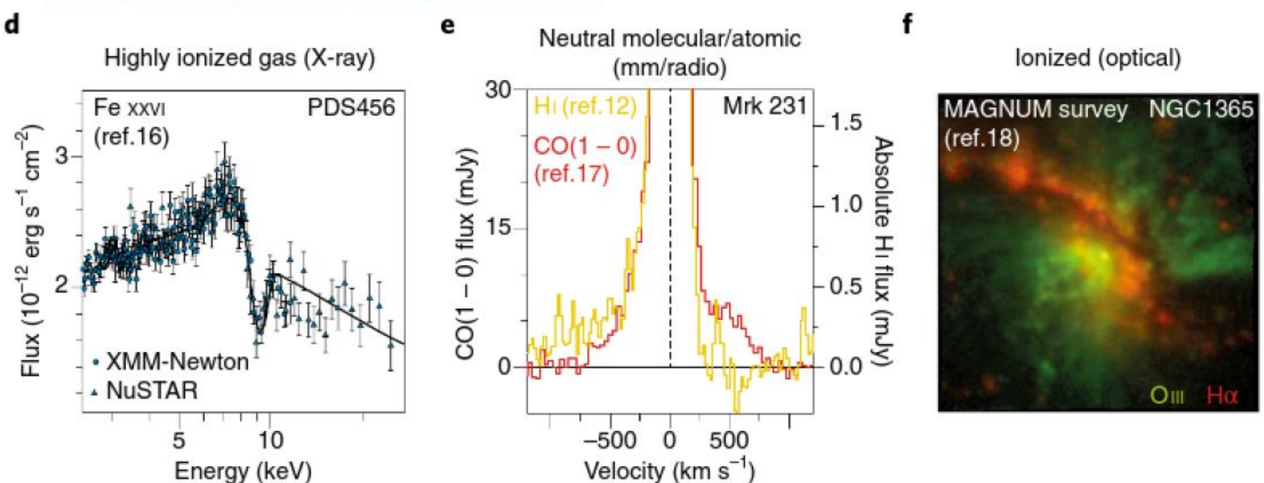

- Difficulties

Quasar spectroscopy

Analysis of the absorption lines in Quasar spectra is a powerful method to study intergalactic and interstellar medium in the early Universe.

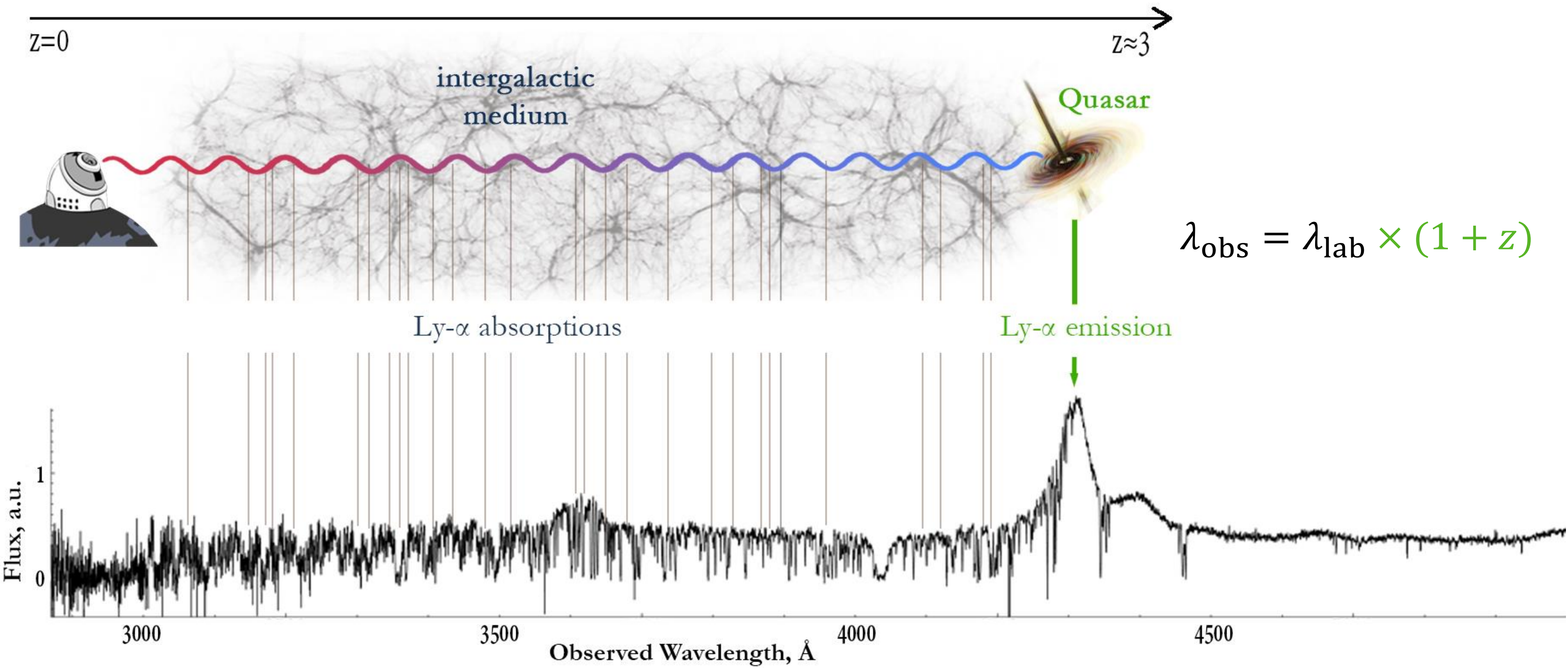

$$\lambda_{\mathrm{obs}} = \lambda_{\mathrm{lab}} \times (1+z)$$

Quasar spectroscopy. DLA systems

In some cases (**~15%)** there is a damped Lya line in the spectrum

Damped Lyman Alpha (DLA) system: $\log N(\mathrm{HI}) \gtrsim 20$ (N – column density [cm^{-2}])

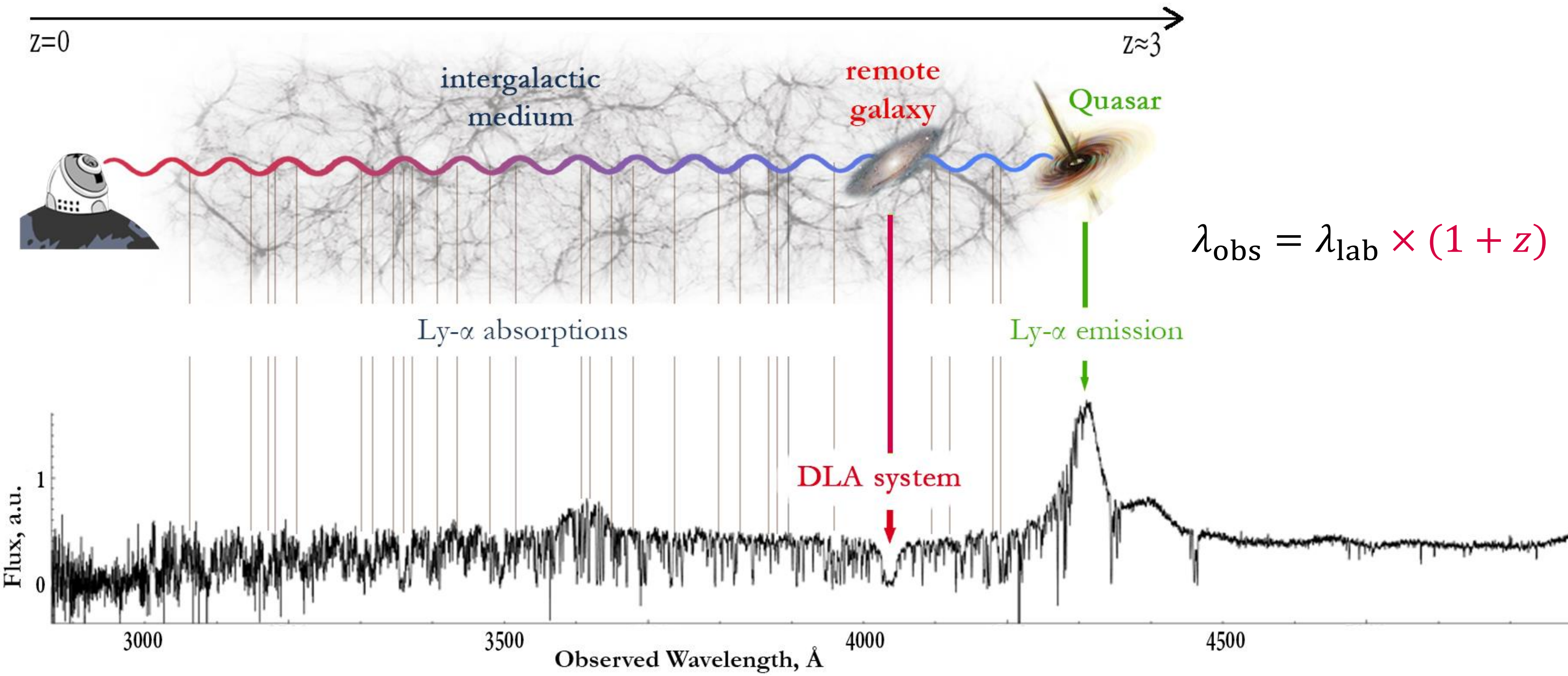

$$\lambda_{obs} = \lambda_{lab} \times (1 + z)$$

Quasar spectroscopy. H_2-bearing DLAs

In **~5%** of intervening DLA systems (SB & Noterdaeme 2018) one can detected the absorption lines of **H_2 molecules** (and in some case HD and CO).

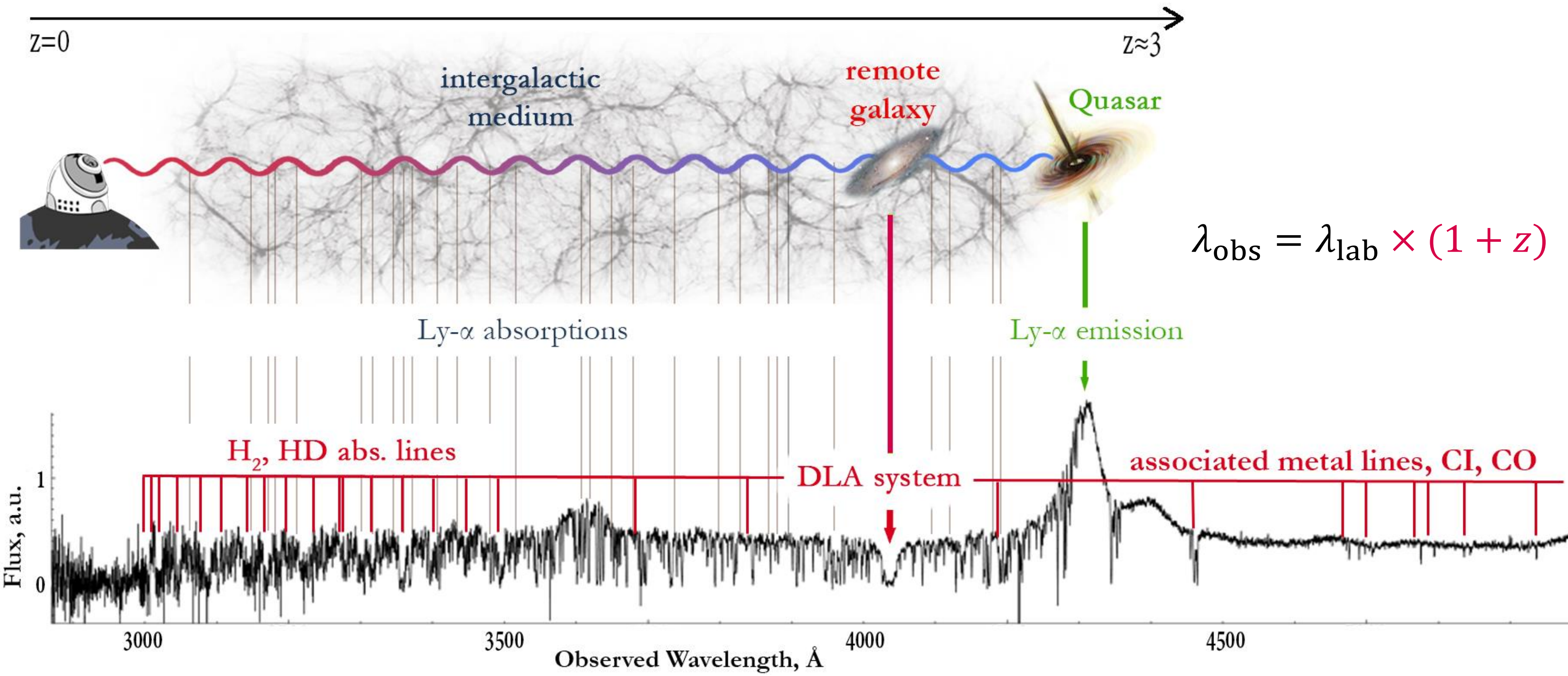

$$\lambda_{\rm obs} = \lambda_{\rm lab} \times (1 + z)$$

Molecular hydrogen (in absorption)

- H_2 is the most abundant molecule, but it is very hard to detect in emission.

- Can be detected **in absorption** using **Lyman** and **Werner** bands:

Balashev+19

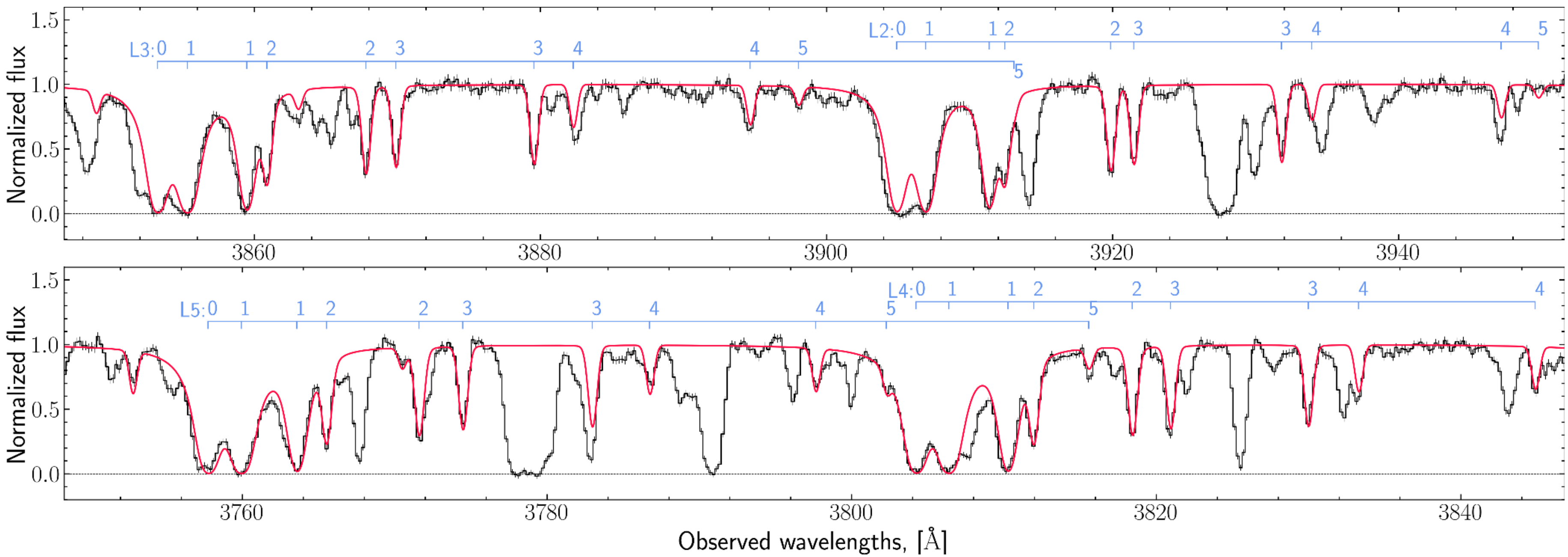

- Several rotational levels usually are detected

$\Longrightarrow$ constrain on the **physical conditions** (temperature, density, UV field, …)

Molecular hydrogen. Physical conditions in CNM

Observed rotational levels of H_2 are populated by **UV pumping** and **collisions**

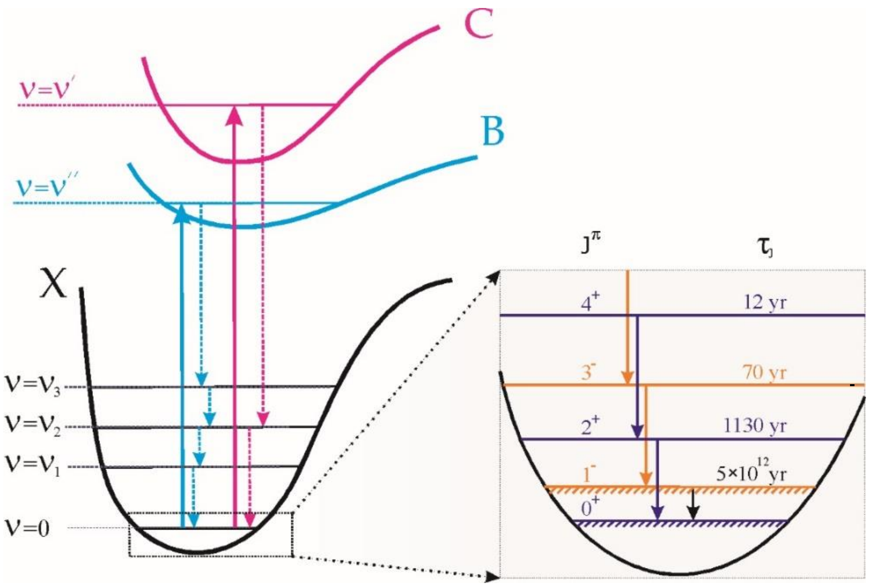

⇒

Klimenko,SB20

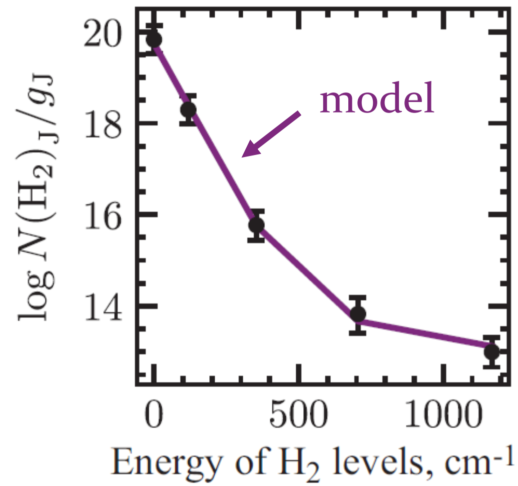

⇓

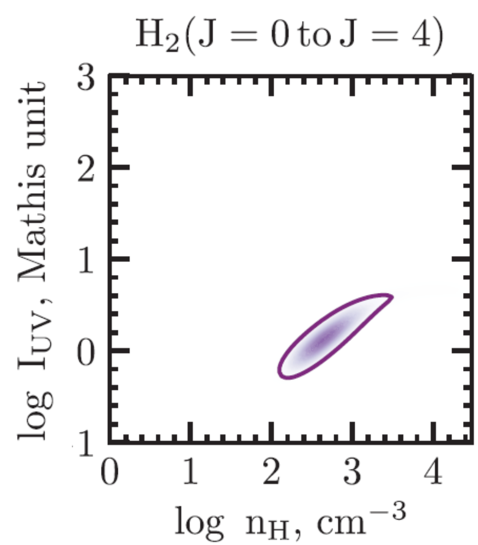

Modeling of the population of rotational levels of H_2 allow us to estimate:

- **temperature** (orto-para ratio of H_2)
- **number density**
- **UV flux**

} ⇒ **Thermal pressure**

Proximate absorption systems

What if an absorption system is located near QSO?

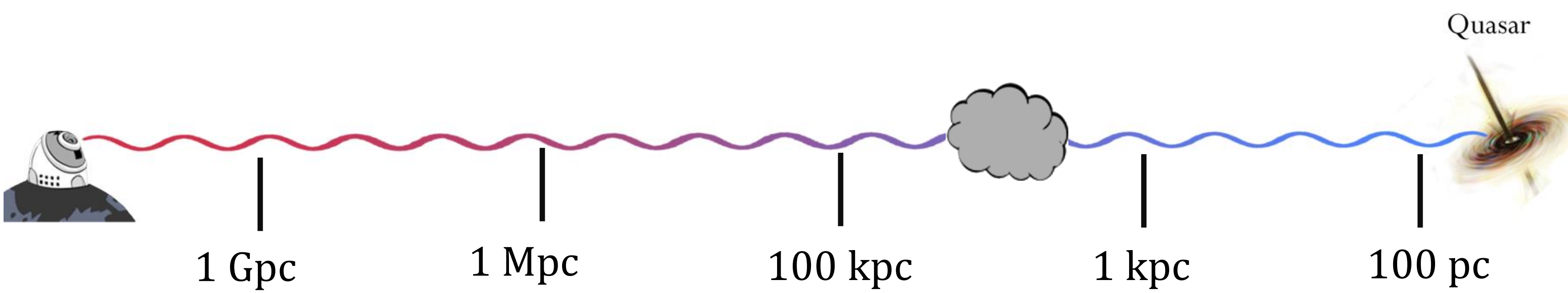

- Changes in the external conditions:
  - enhanced radiation background
  - mechanical impact by Active Galactic Nuclei feedback

- Changes in the incidence rate of absorption systems:

Clusterization or QSO impact

Proximate absorption systems

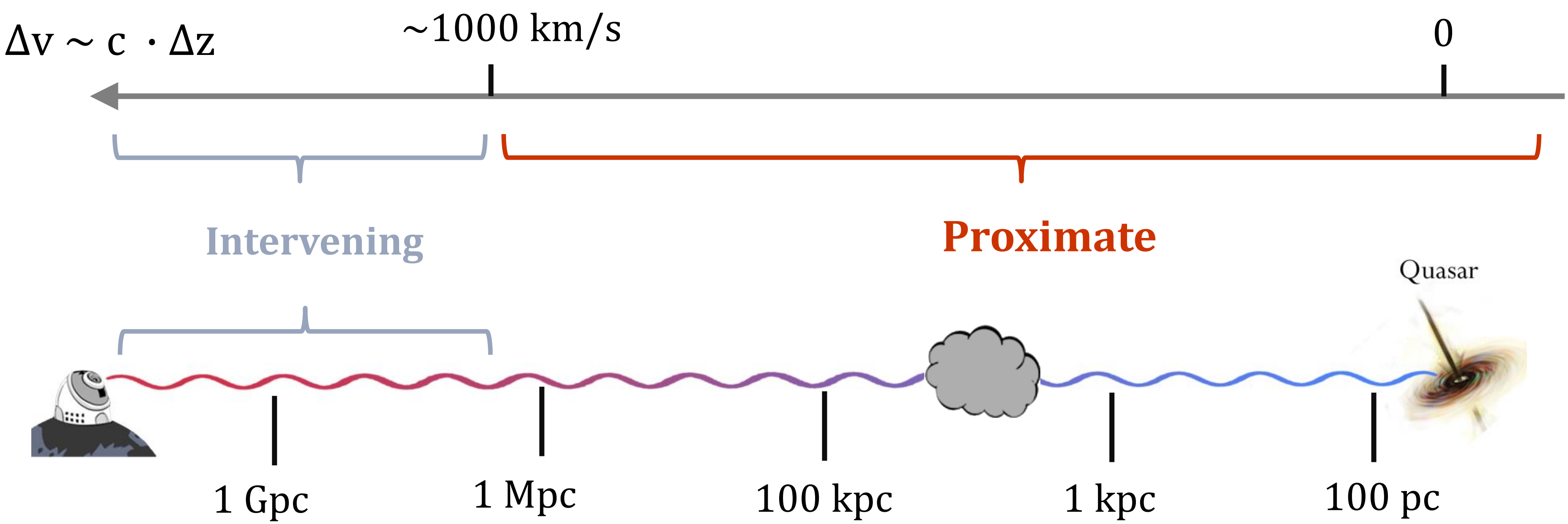

Proximate absorption systems

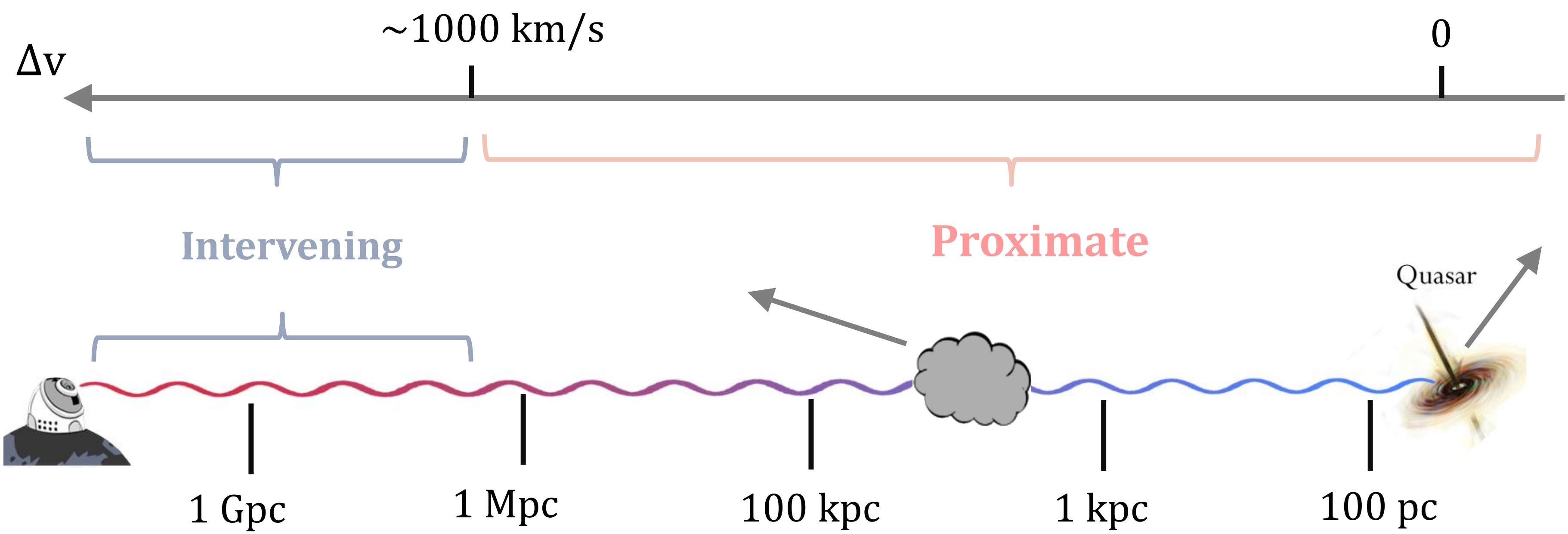

Unknown peculiar velocities of both absorption system and QSO did not allow us to constrain the distance using the redshift measurements.

However, some species, e.g. **molecular hydrogen**, allow us in principle to constrain external UV field, which can be used to constrain the distance to the central engine.

Proximate H_2-bearing DLAs

Using SDSS we found a population of proximate H_2–bearing DLAs at z>2.5

- **Incidence rate** is significantly **>5 times** higher than for intervening DLAs
- ~ in 50 % of these systems we see and extended Lya emission in the DLA core.
- this subsample with Lya leakage is likely related to the **quasar outflows**

Noterdaeme,SB+19

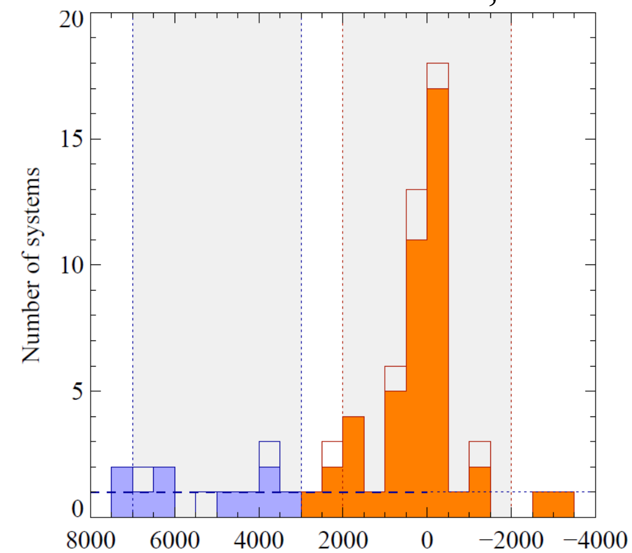

$$\Delta v[\mathrm{km\ s^{-1}}] \approx c\,\frac{z_{\mathrm{QSO}} - z_{\mathrm{abs}}}{1 + z_{\mathrm{QSO}}}$$

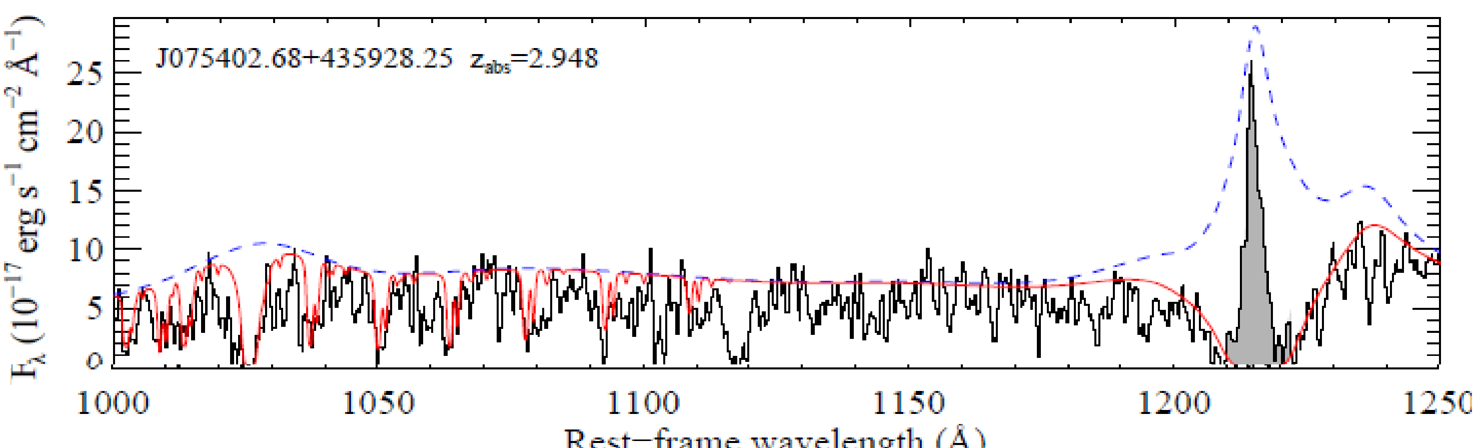

Proximate DLAs. Lya leakage

Lya can be emitted from the very extended region around QSO (e.g Borisova+2018)

Spectrum

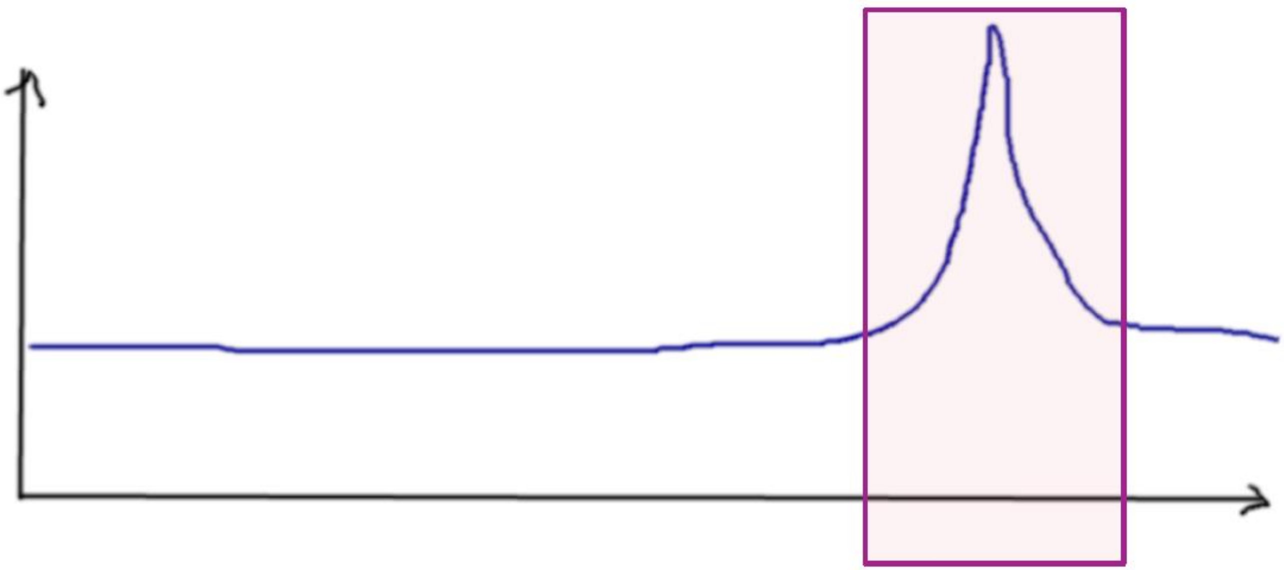

Image

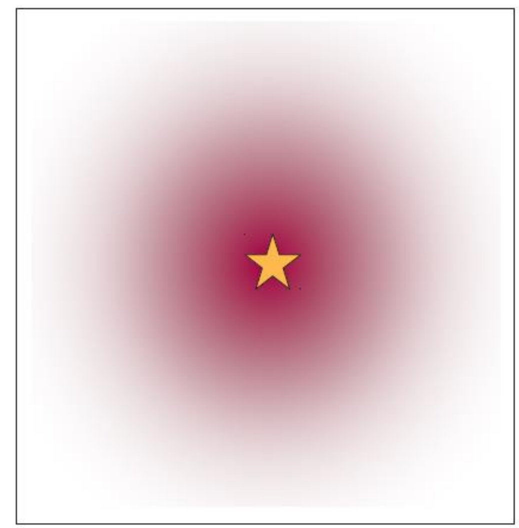

- Yellow star – QSO continuum source – scales: < pc
- Red area – Lya emission – scales: ~ pc – 100 kpc

Proximate DLAs. Lya leakage

If extent of absorption system is less than the size of Lya emission region, some parts of Lya leak, which results in the Lya emission line at the bottom of damped absorption profile.

Spectrum

Image

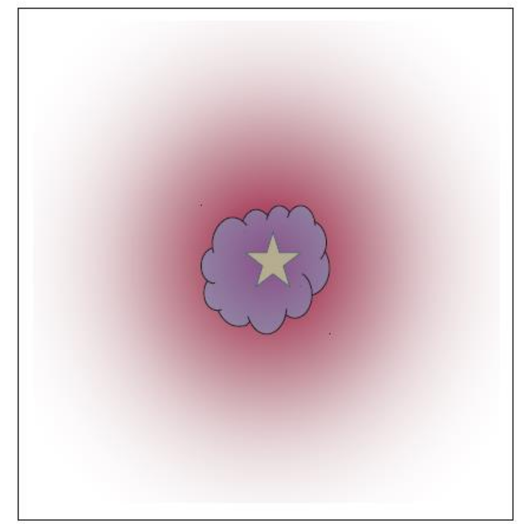

- Yellow star – QSO continuum source – scales: < pc
- Red area – Lya emission – scales: ~ pc – 100 kpc
- Blue area – absorbing cloud – scales: ~ kpc

Proximate H_2-bearing DLAs. Follow-up observations

Noterdaeme, SB, et al. 2019

Table 1. Sample of strong proximate H_2 absorbers in SDSS.

RA (J2000)	Dec (J2000)	MJD-plate-fiber [a]	z_{H2}	log N(H I) (cm^{-2})	log $N(H_2)$ [b] (cm^{-2})	A_V [c] (mag)	$F_{Ly-\alpha}$ (10^{-17} erg s^{-1} cm^{-2})	f_{leak} [d]	Flag [e]
00:15:14.82	18:42:12.34	56270-06111-0908	2.628	20.85	19.8	0.09	49.7 ± 1.9	0.19	3 A
00:19:30.55	−01:37:08.46	55536-04366-0874	2.529	21.00	20.0	0.03	4.5 ± 1.9	0.02	3 A
00:46:05.89	00:43:27.81	55444-04222-0981	2.940	20.00	19.3	0.10	-0.4 ± 0.8	0.00	0 A
00:59:17.64	11:24:07.70	56165-05706-0118	3.034	21.75	19.0	0.07	12.4 ± 2.4	0.04	1 A
01:02:11.89	02:52:07.18	57281-07858-0826	2.657	20.80	19.5	−0.00	-0.5 ± 1.5	0.00	0 A
01:25:55.11	−01:29:25.00	56898-07877-0966	2.665	21.75	20.2	0.17	70.0 ± 5.0	0.27	2 A
01:26:54.45	11:38:23.29	55831-04669-0080	2.603	20.50	19.2	0.04	21.3 ± 1.3	0.07	3 A
01:36:44.02	04:40:39.10	55508-04274-0691	2.779	20.75	19.5	−0.04	1.6 ± 1.3	0.01	3 A
02:16:02.33	04:13:57.35	55486-04266-0012	2.661	20.55	19.7	−0.34	16.3 ± 1.4	0.12	3 A
02:19:26.55	−01:10:57.30	55478-04237-0364	2.812	20.00	19.0	0.42	7.9 ± 0.6	0.23	0 B
02:23:16.90	−03:07:21.42	56904-07832-0378	2.583	22.00	20.0	0.01	23.9 ± 3.6	0.08	3 A
07:54:02.68	43:59:28.25	57067-08276-0092	2.948	21.40	19.5	0.22	71.6 ± 3.0	0.36	3 A
07:56:34.69	11:23:30.35	55602-04511-0874	3.315	21.00	20.1	−0.15	1.9 ± 1.7	0.03	3 A
07:59:01.28	28:47:03.43	55535-04453-0850	2.822	21.30	19.5	−0.03	15.6 ± 1.6	0.04	3 A
08:03:51.64	50:03:17.65	56992-07317-0693	2.977	20.65	19.0	0.62	3.6 ± 1.0	0.03	0 A
08:07:57.45	51:52:34.24	56741-07377-0768	3.124	21.00	19.3	0.11	8.8 ± 1.4	0.10	0 A
08:16:14.21	03:58:19.77	55869-04763-0096	3.682	20.00	19.0	−0.00	5.9 ± 1.4	0.08	3 B
08:21:26.13	36:26:06.10	57449-08857-0340	2.597	21.30	19.3	−0.01	-4.0 ± 2.3	0.00	3 A
08:55:02.19	42:09:37.16	57375-08296-0646	2.719	22.30	19.8	−0.16	-3.6 ± 3.8	0.00	3 A
08:58:59.67	17:49:25.19	55913-05297-0566	2.625	20.40	19.8	0.05	-0.5 ± 1.5	0.00	3 A

...

P103 (2018 year) → 32 hrs VLT/ 9 systems (rank B) → 5 hours (**J0015+1842**)

P105 (2019 year) → 27 hrs VLT/ 9 systems (rank A) → 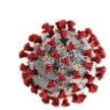

J0015+1842

+

SDSS Image:

Regular / “boring” qso

VLT / X-shooter:

4hrs observation
+ perfect conditions (0.8” – 0.5”)

⇓

(Noterdaeme, SB, et al. 2021)

J0015+1842. X-shooter spectrum

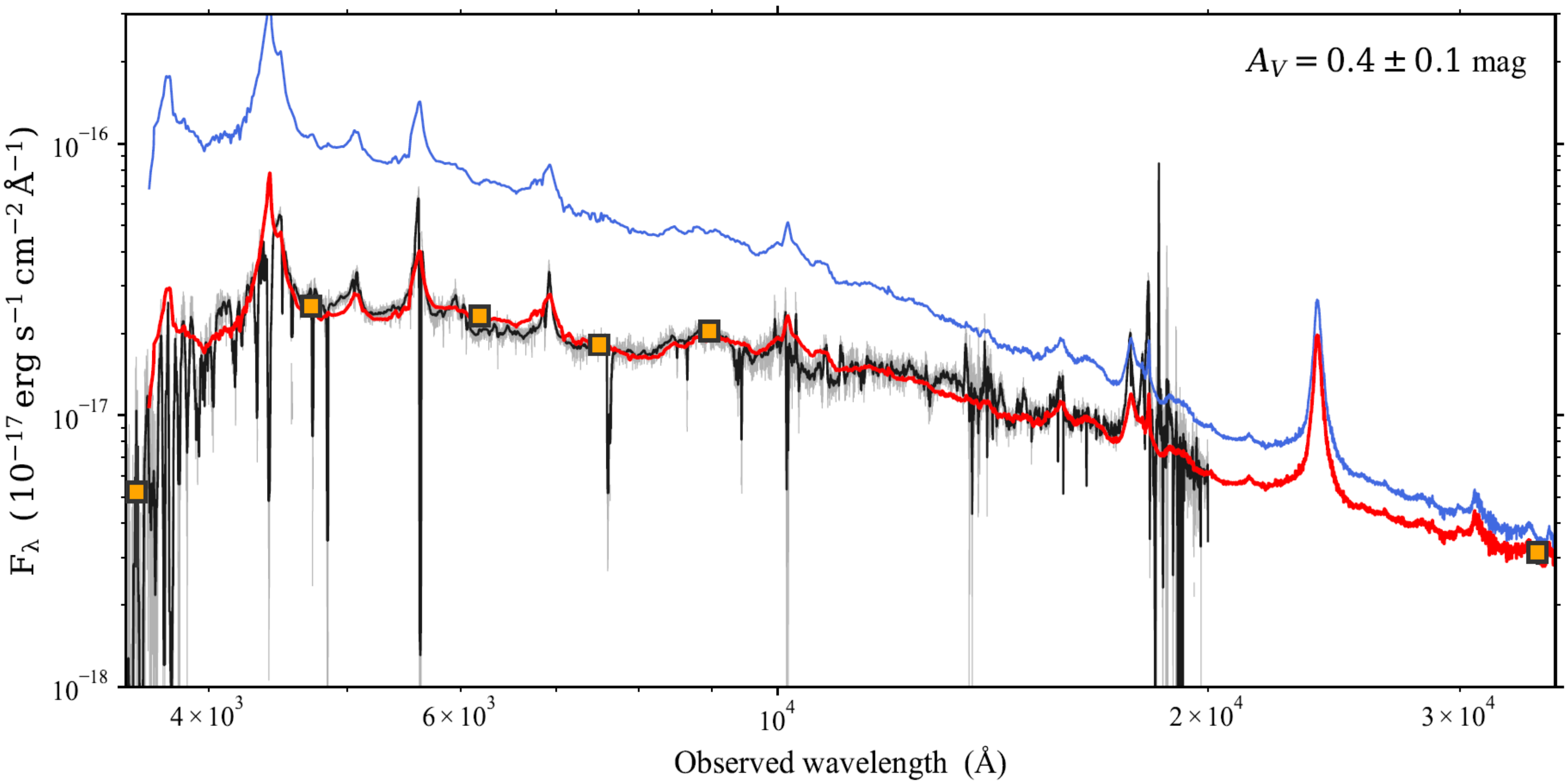

J0015+1842. [OIII]

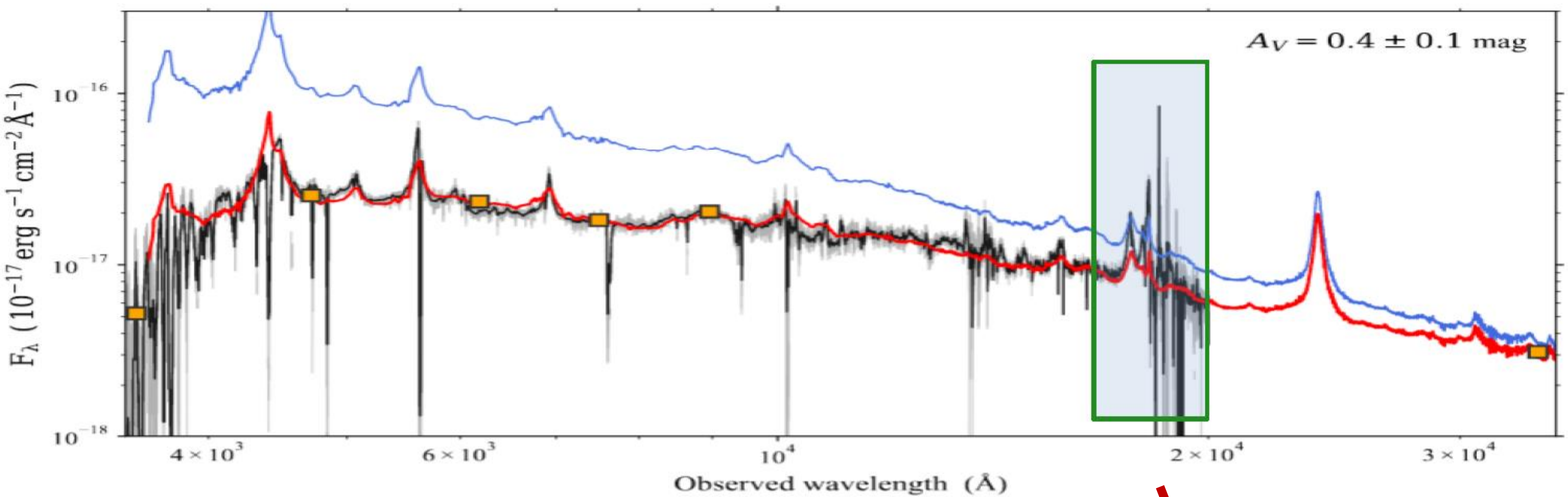

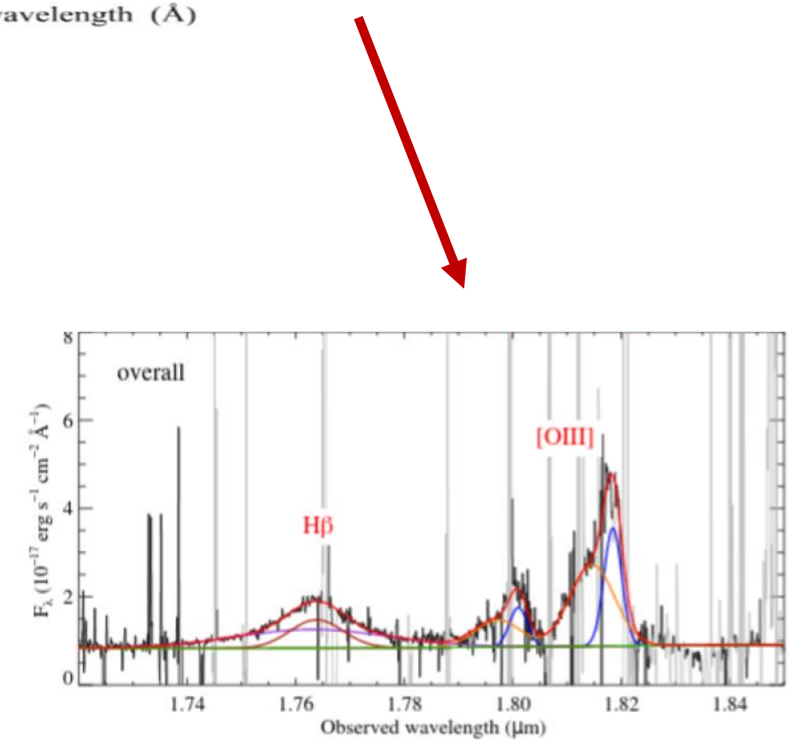

J0015+1842. [OIII]

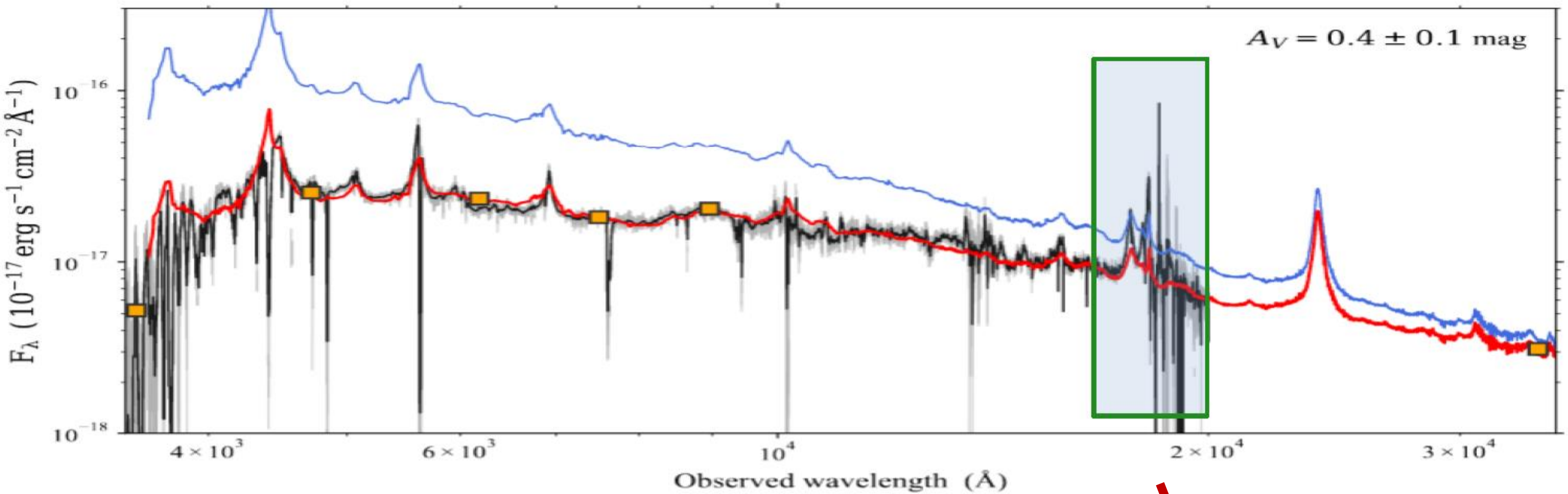

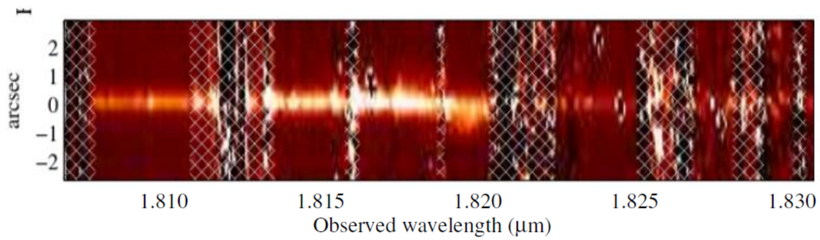

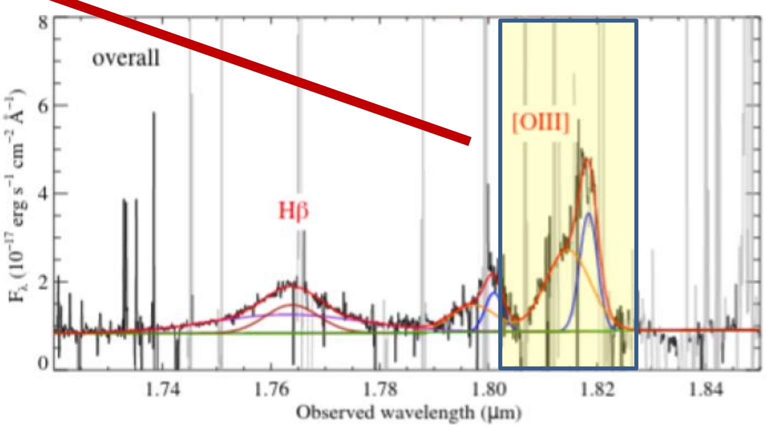

J0015+1842. [OIII]

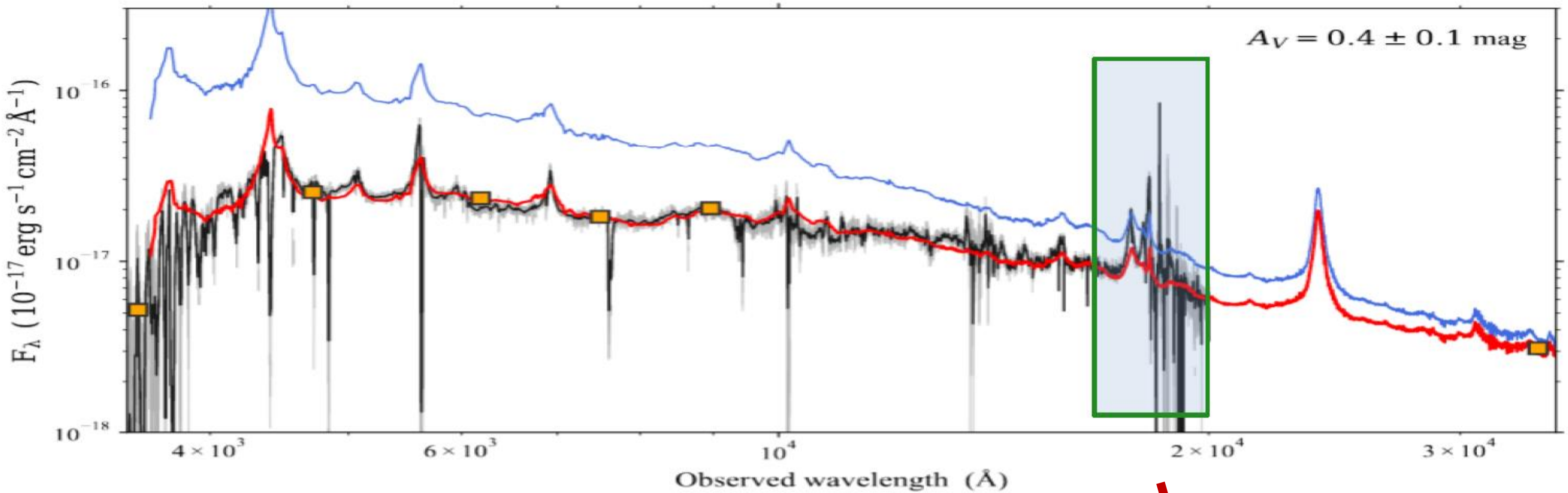

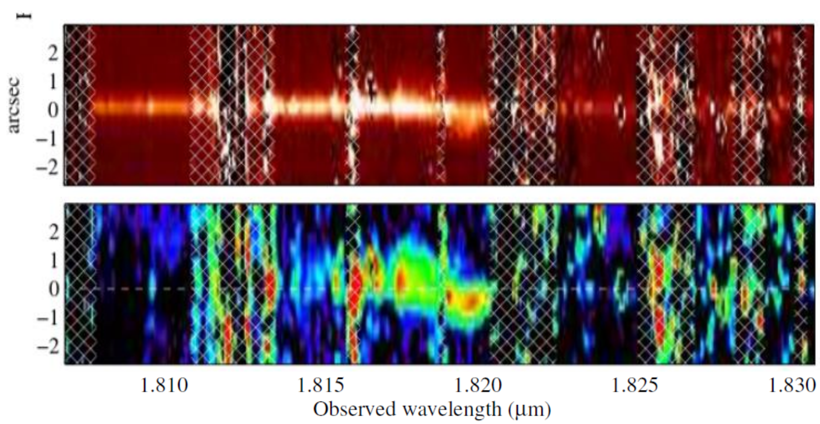

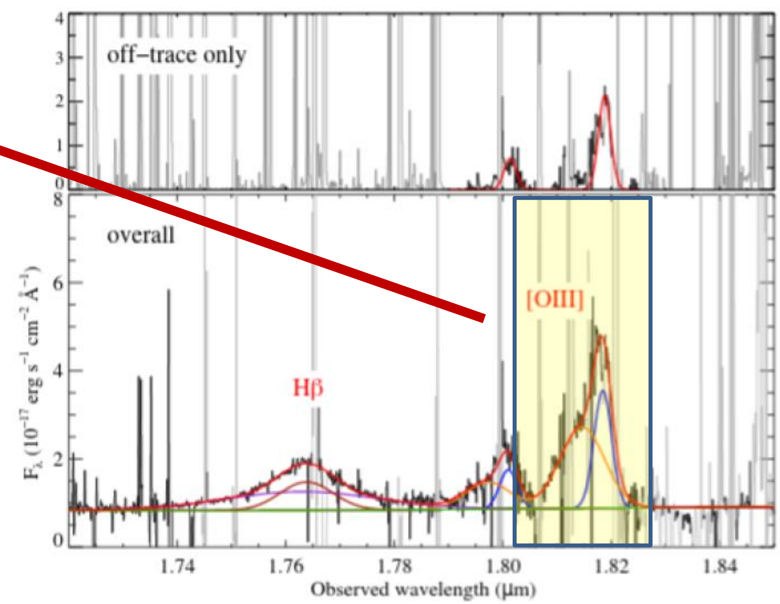

Extended emission in [OIII] line (several kpc)

J0015+1842. Lya emission

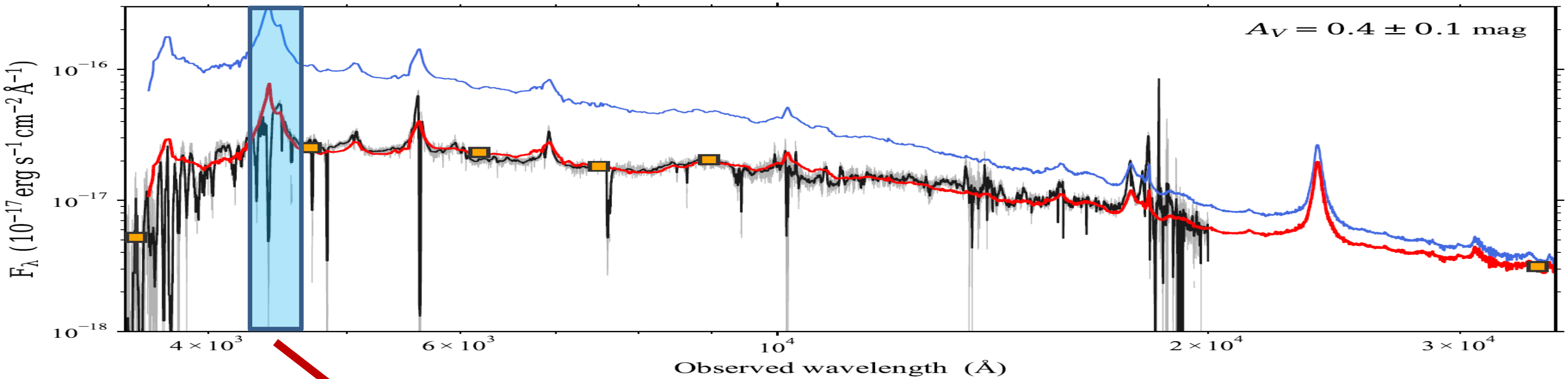

Lya emission/absorption

In 1d spectrum:

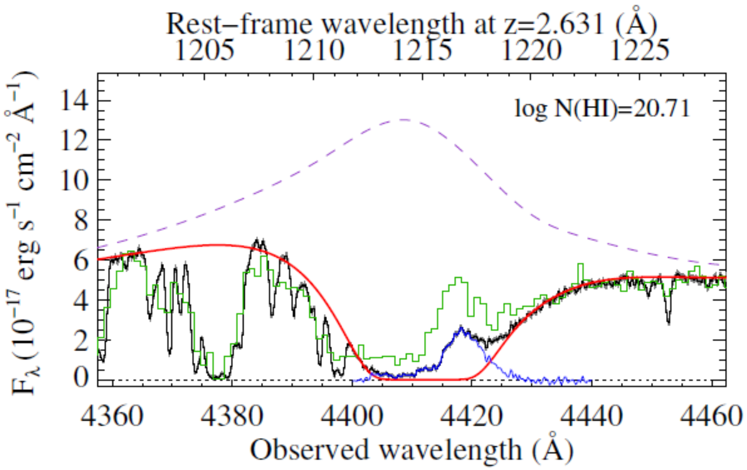

In 2d spectrum:

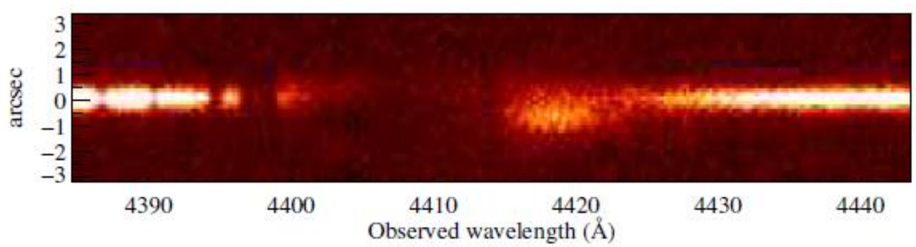

Extended emission in Lya line (several kpc)

J0015+1842. Absorption lines

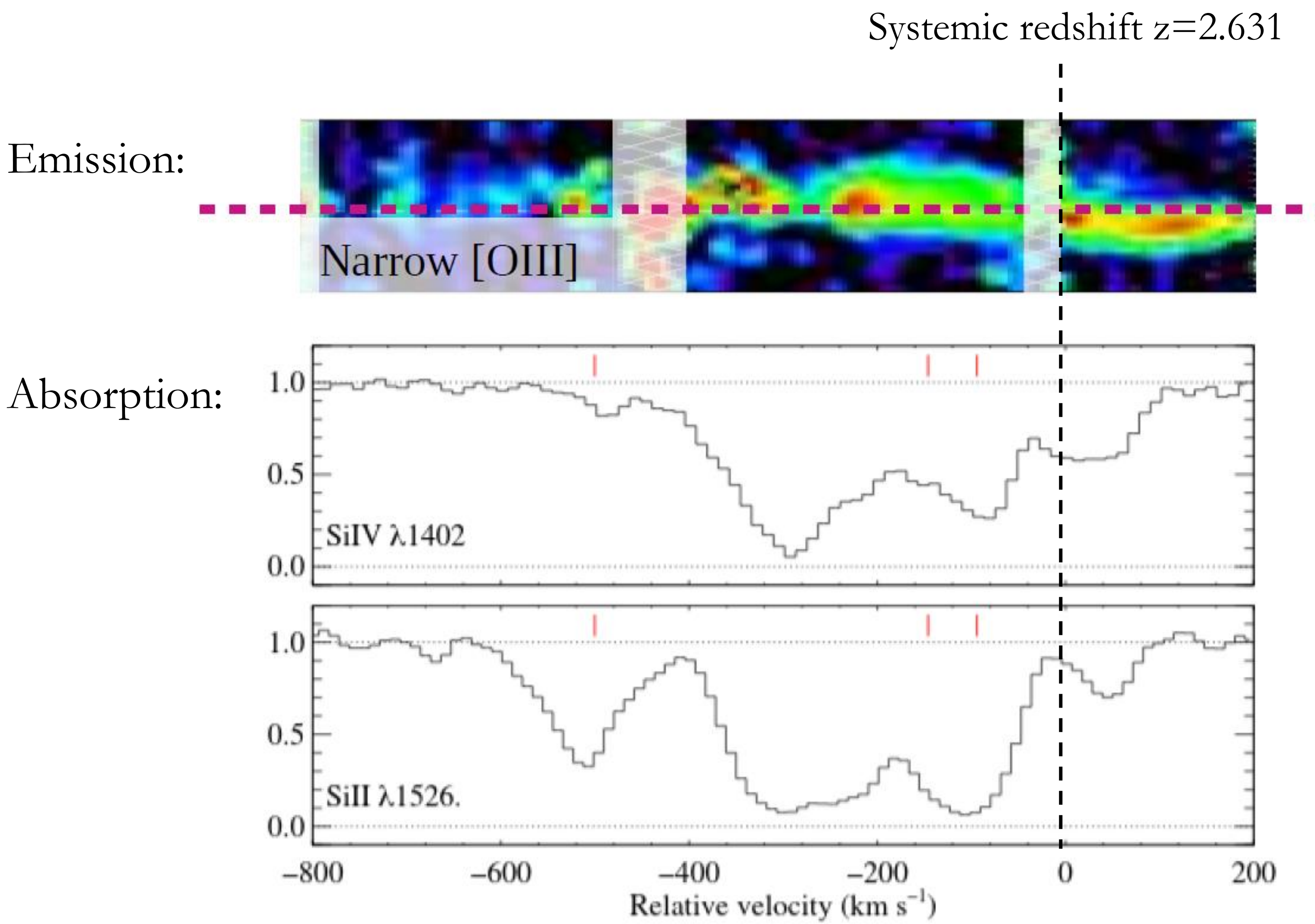

J0015+1842. H_2 absorption lines

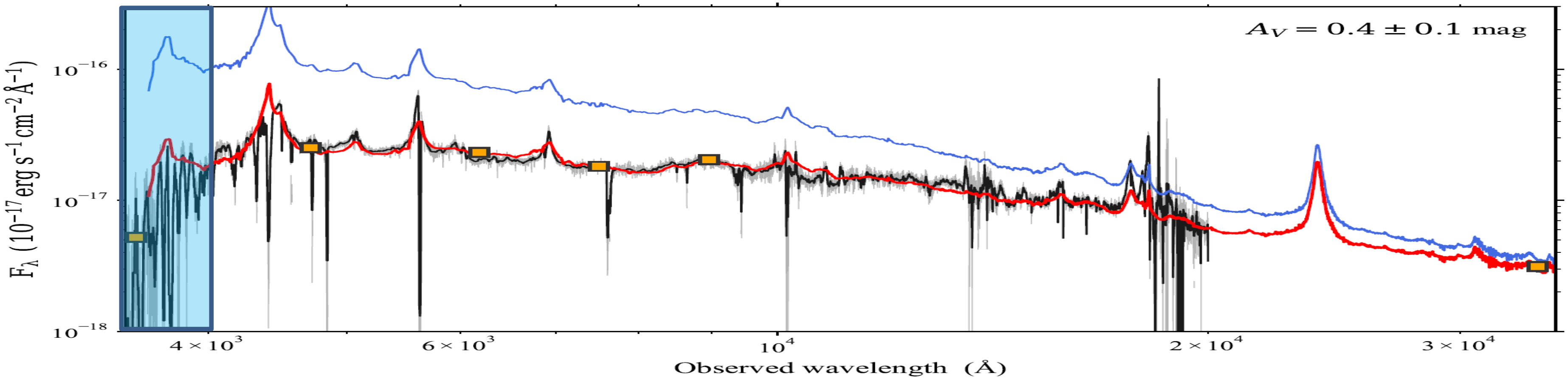

J0015+1842. H_2 absorption lines

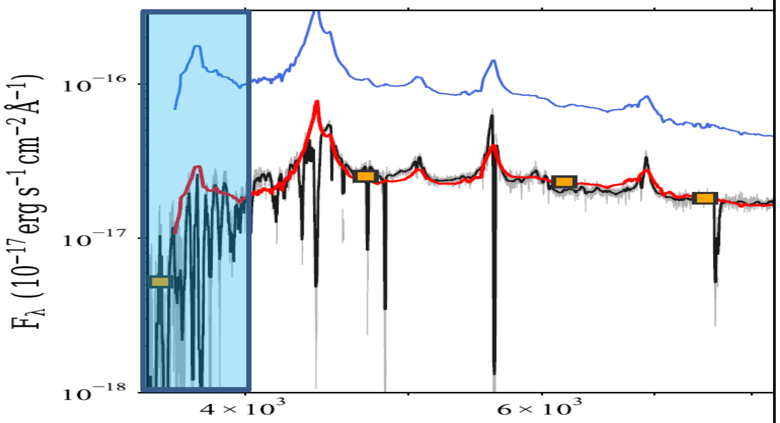

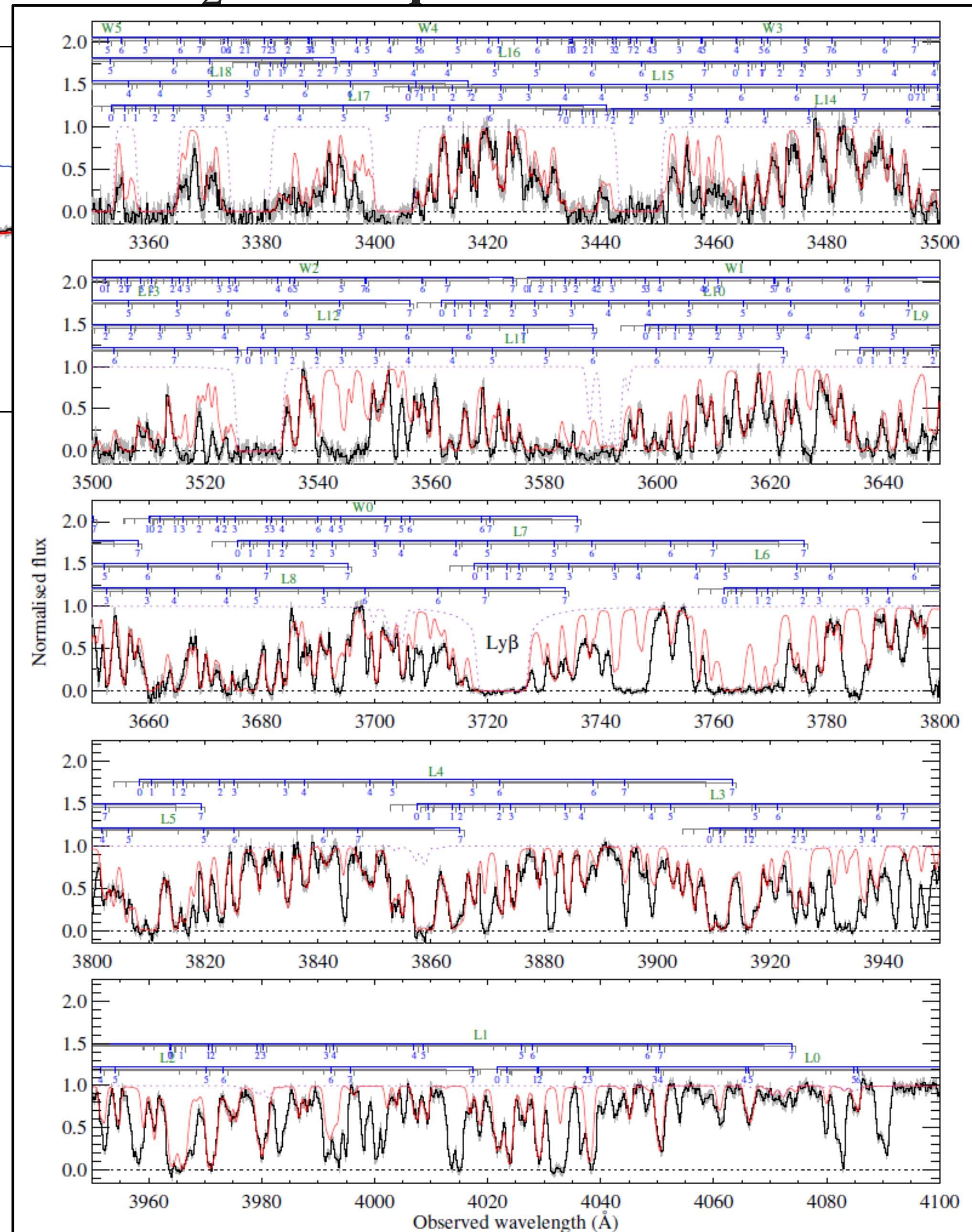

We see significantly enhanced excitation of H_2 rotational levels in comparison with the regular intervening systems

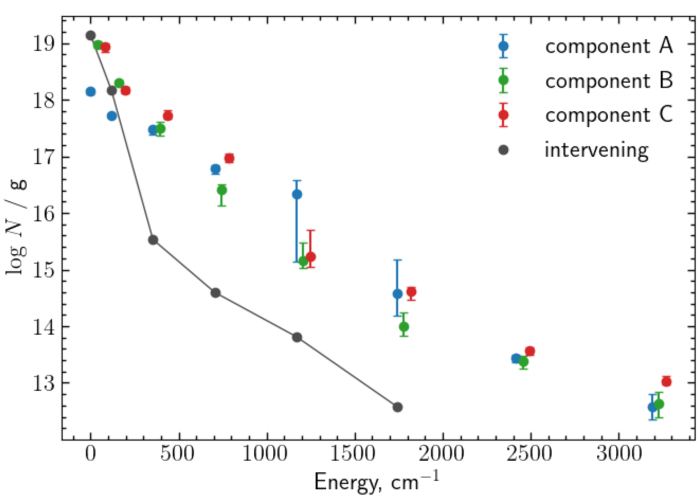

J0015+1842. H_2 absorption lines

Modeling of the H_2 rotational level population:

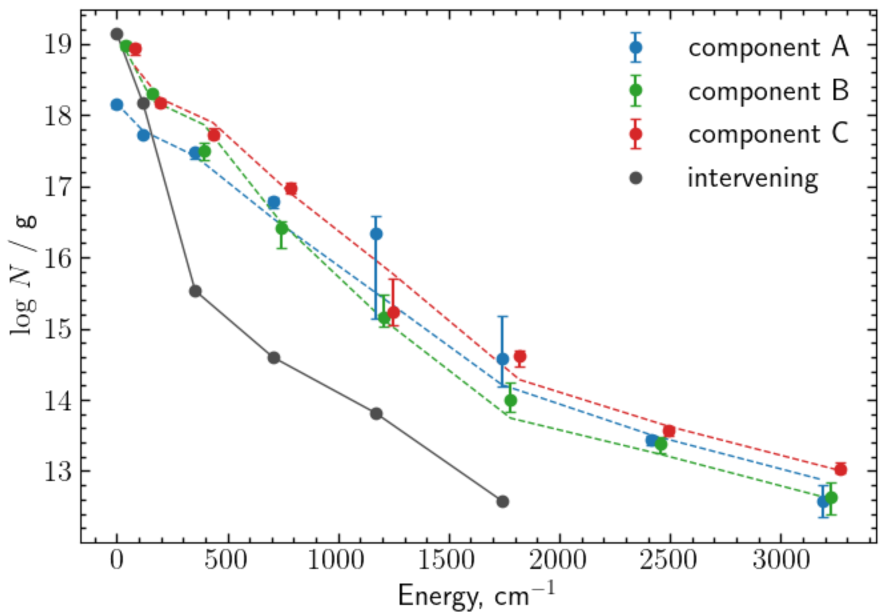

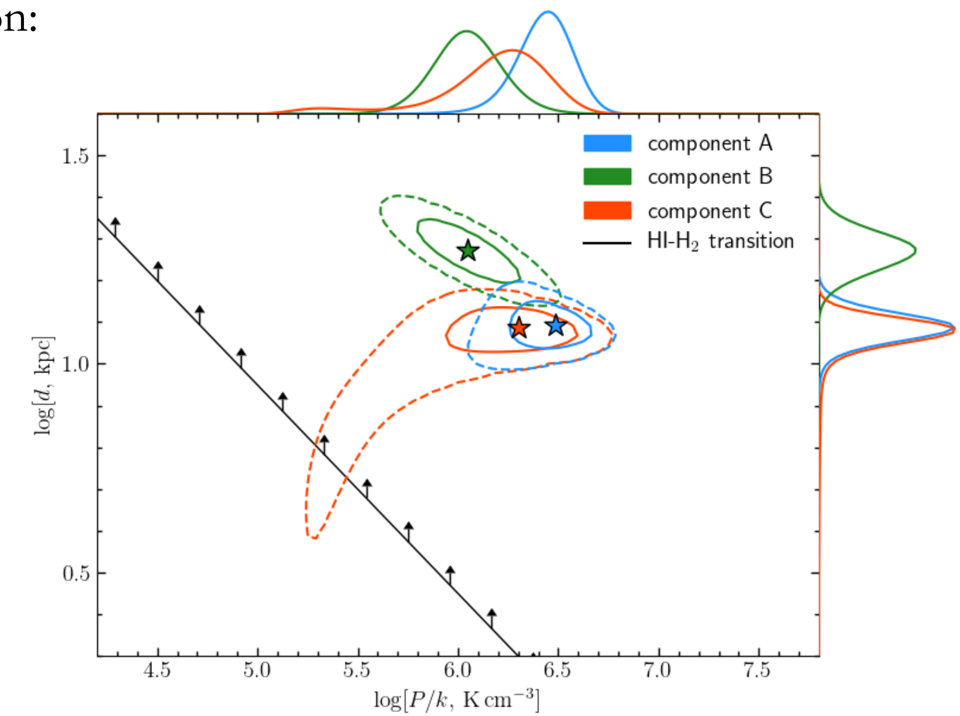

Results:

UV ~ 10^3 Draine field (d = 10 – 20 kpc)
T ~ 100-200 K
log n [cm^{-3}] ~ 4-5

⇒ Typical conditions for the Photodissociation regions (PDR)

J0015+1842. Configuration

Emission and absorption line properties indicated that H_2-bearing gas is associated with the outflow and located ~10 kpc away from central engine.

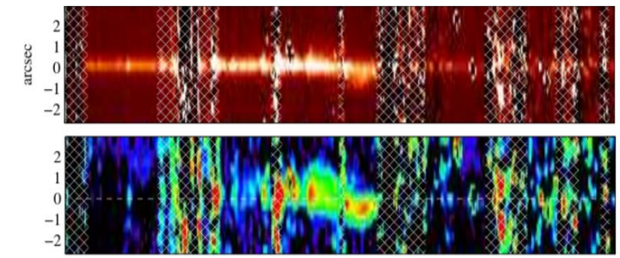

[OIII] emission line with extended emission

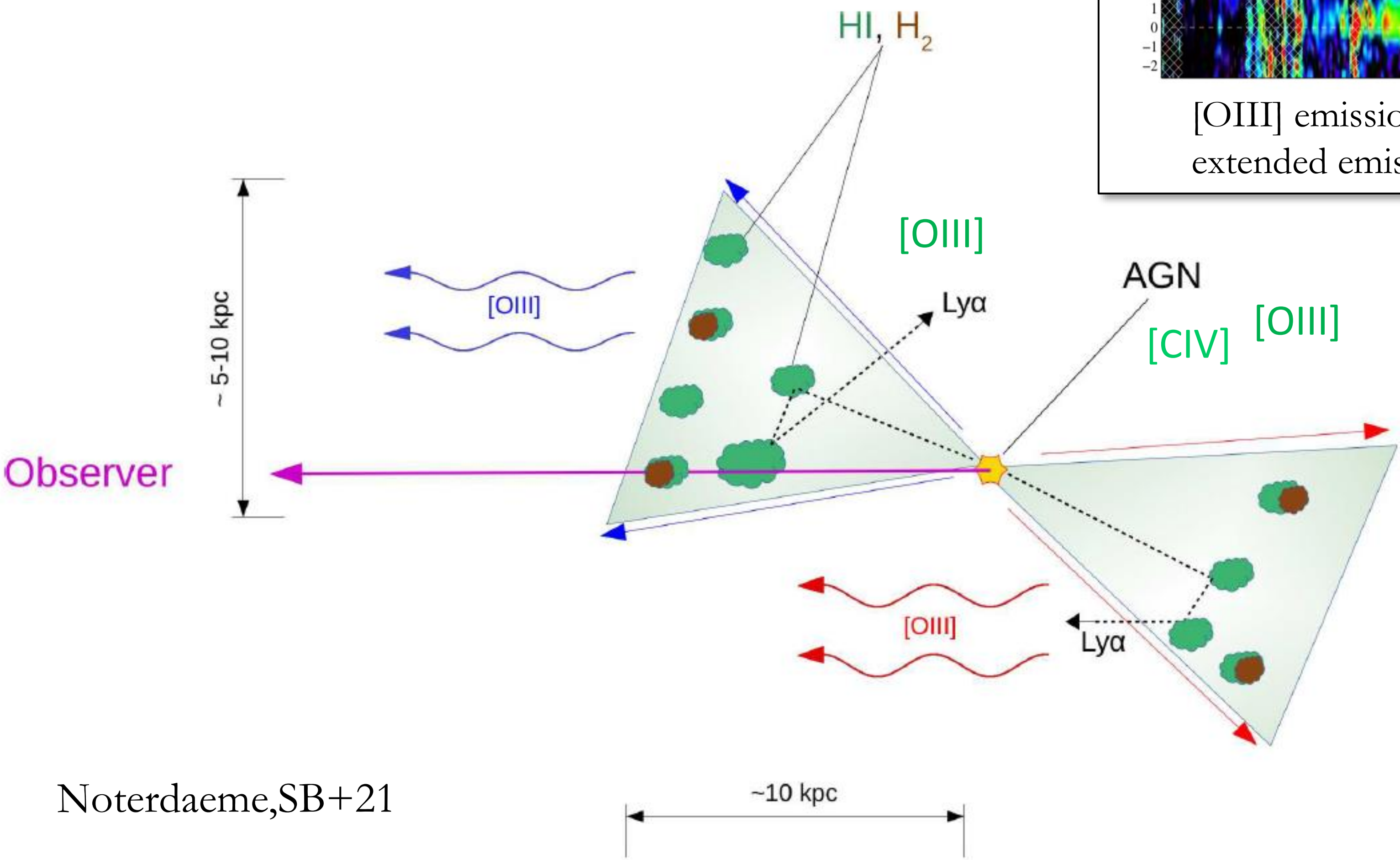

Noterdaeme,SB+21

J0015+1842. Configuration

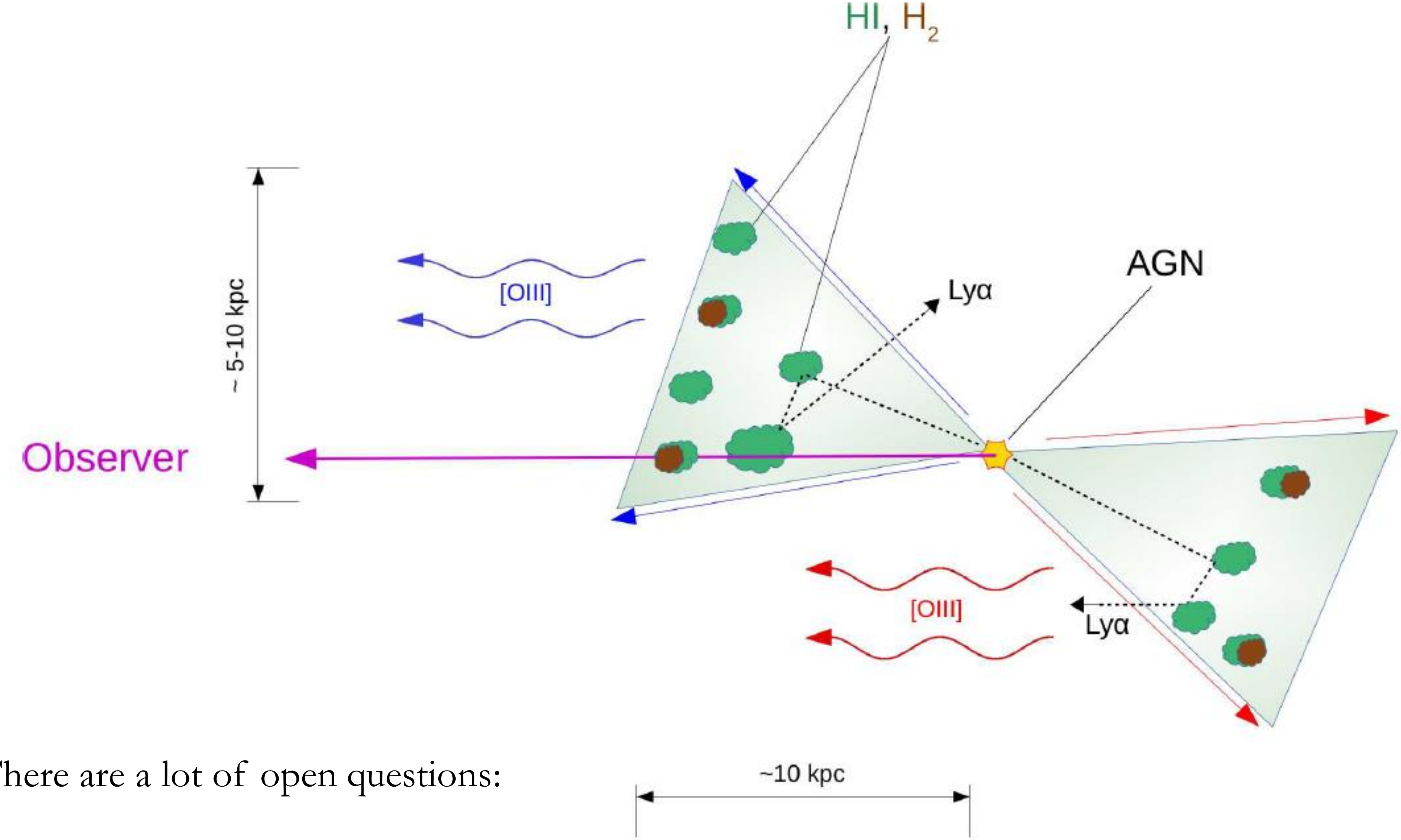

There are a lot of open questions:

- What is the structure of the outflow?
- What are the masses of outflow in different ionization states
- Acceleration of deacceleration of the gas?
- What about the dust?

J0015+1842. H_2 emission from outflow

The H_2 emission from PDR gas in the outflow can be detectable at IR range.

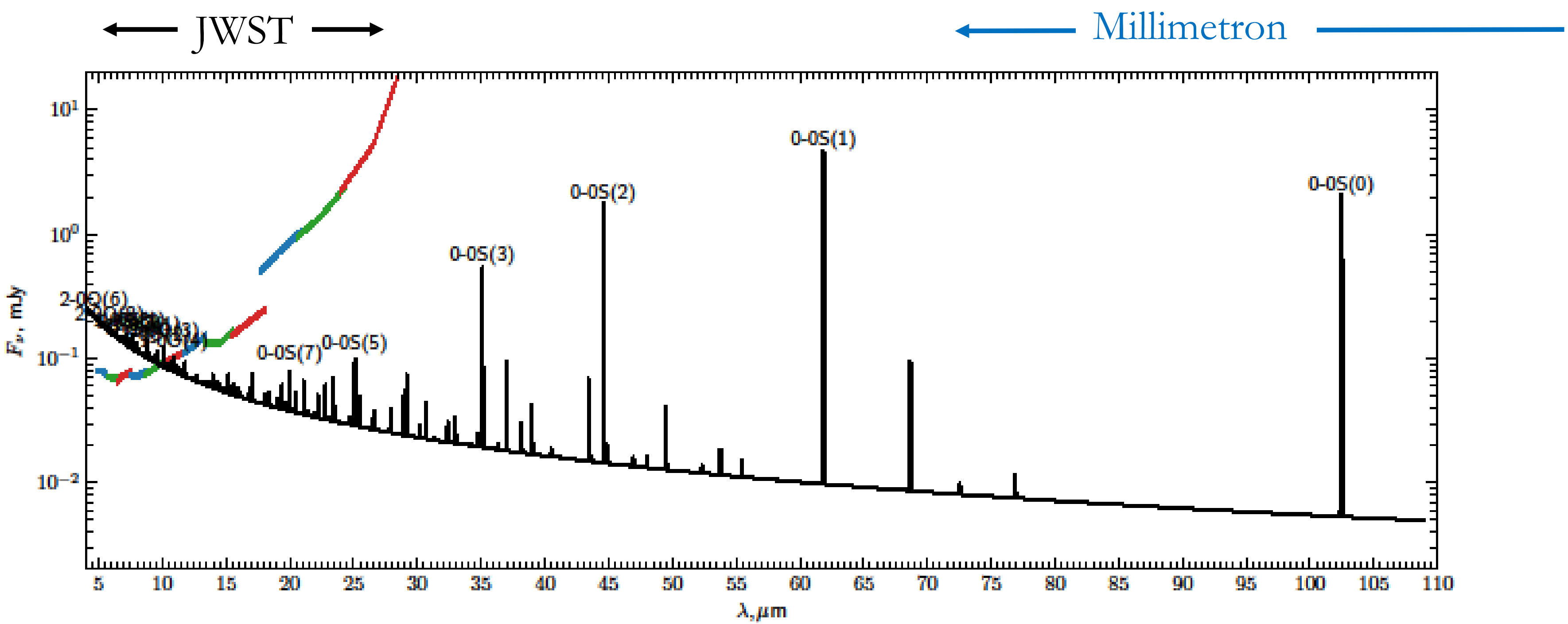

simulated H_2 emission (note, without PAH features + host!)
from 10x10 kpc size outflow ($M_{H2} \sim 10^8 M_\odot$)

… but this is for the z=2.631 (for this particular object), we have targets with z>3

J0015+1842. NOEMA observations

We observed J0015+1842 with NOEMA (ten 15-м antennas: ~80-360 GHz (> 1mm):

Observations:

CO 3-2

95.23 GHz = 345.8 GHz / (1 + 2.631)

~6 hours exposure time

⇒

Noterdaeme,SB+21 (arXiv:2103.09542)

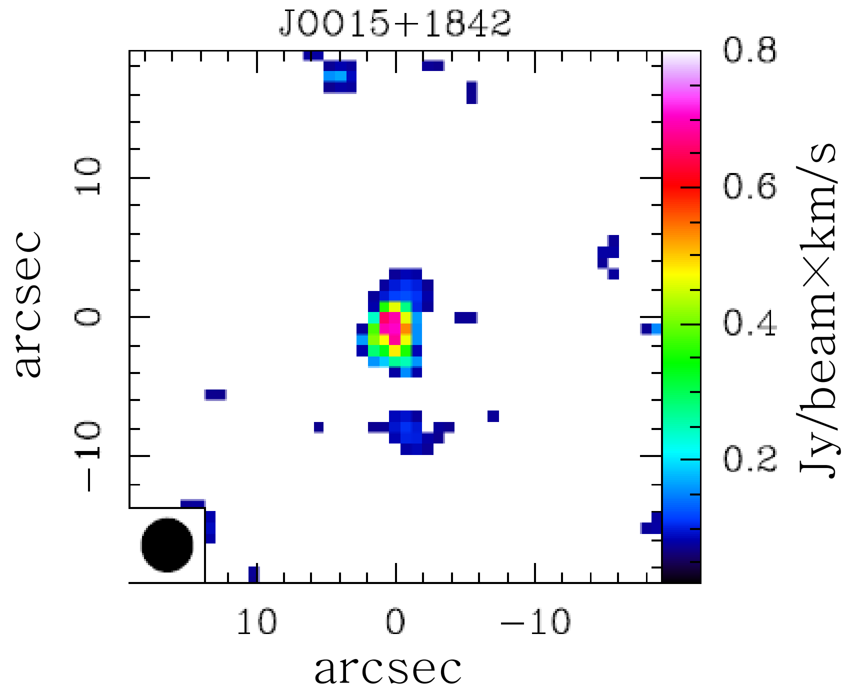

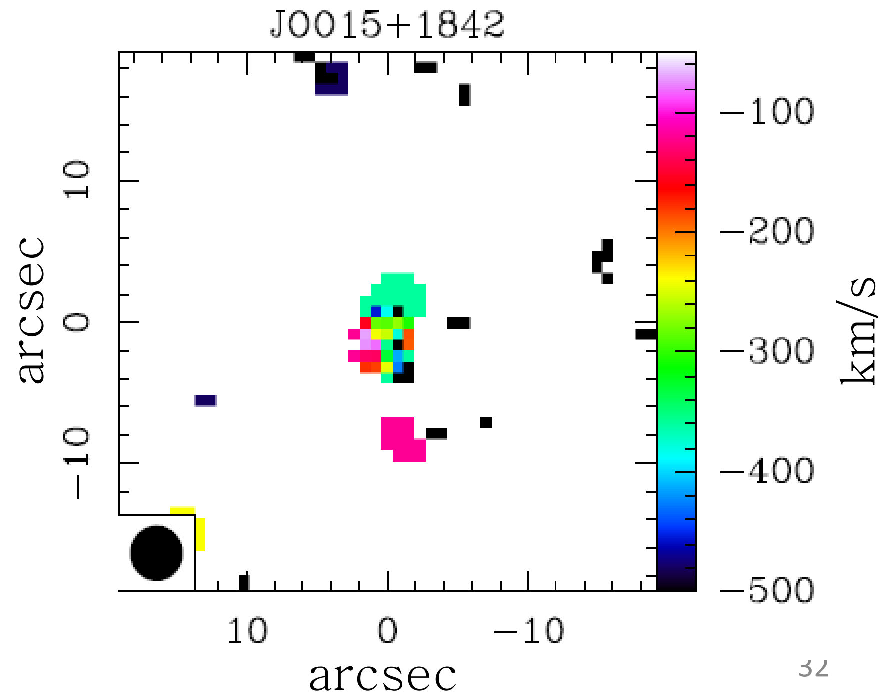

J0015+1842. NOEMA observations

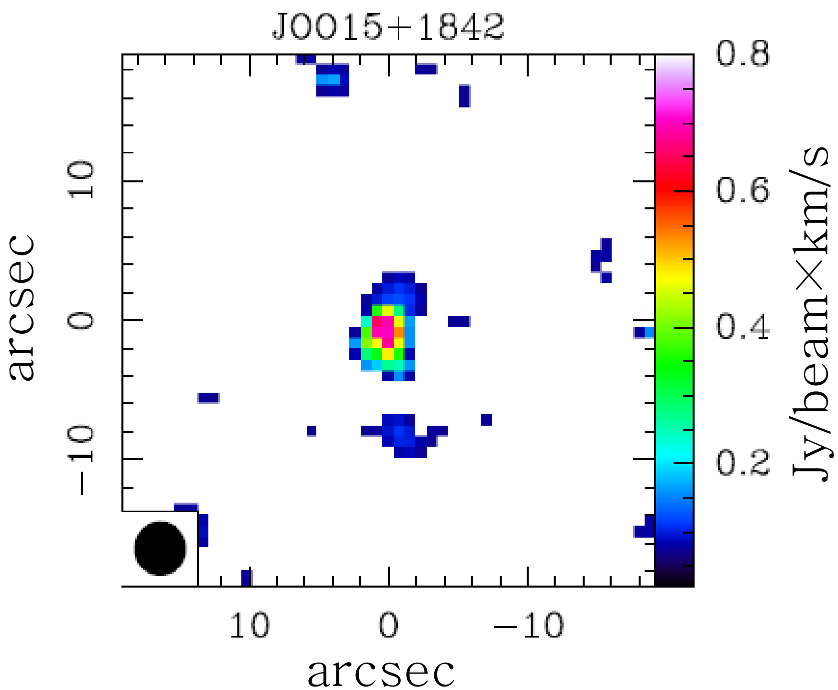

$\Rightarrow$

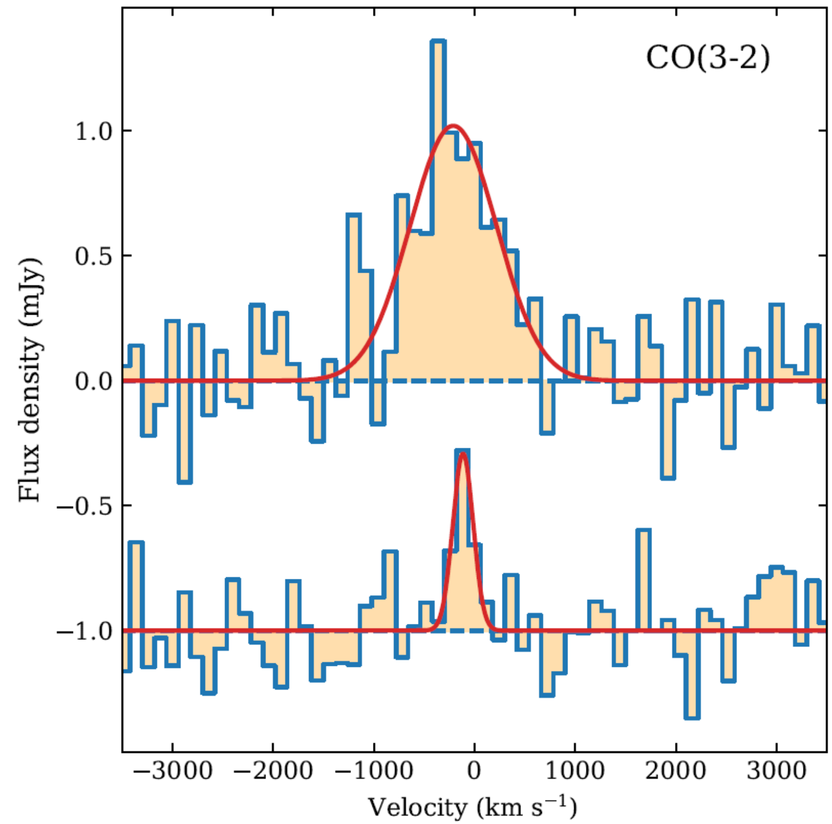

$\Rightarrow \quad S_{\mathrm{CO3-2}}\Delta v = 1.1 \pm 0.1\ \mathrm{Jy\ km\ s^{-1}} \quad \Rightarrow$

$[\alpha_{\mathrm{CO}} = (0.8 - 4) M_{\odot} (\mathrm{km\ s^{-1} pc^{2}})^{-1}] \quad \Rightarrow \quad M_{\mathrm{H2}} = (3 - 17) \times 10^{10} M_{\odot}$

J0015+1842. NOEMA observations

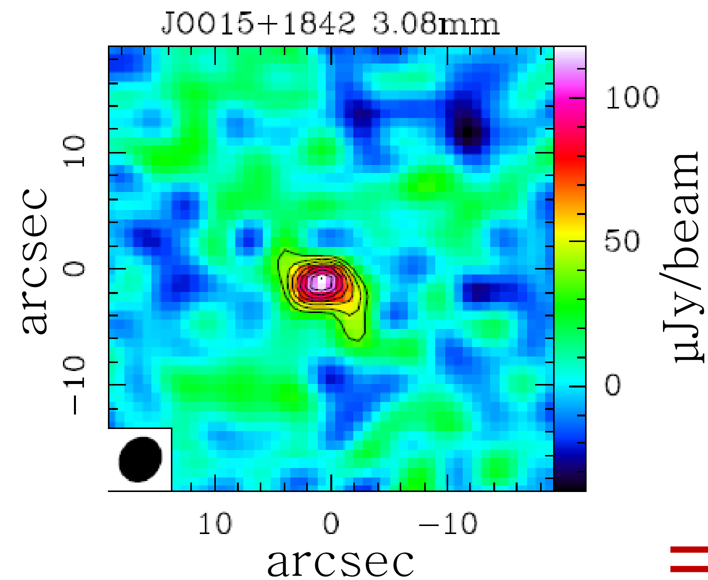

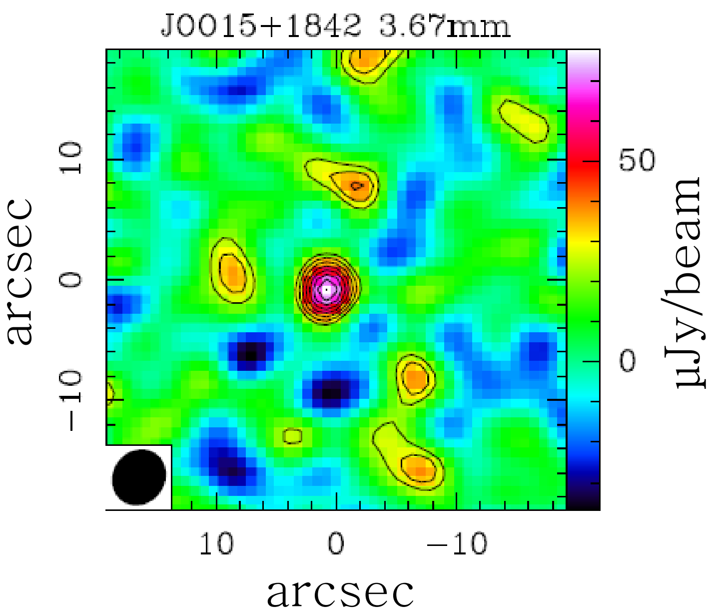

⇒

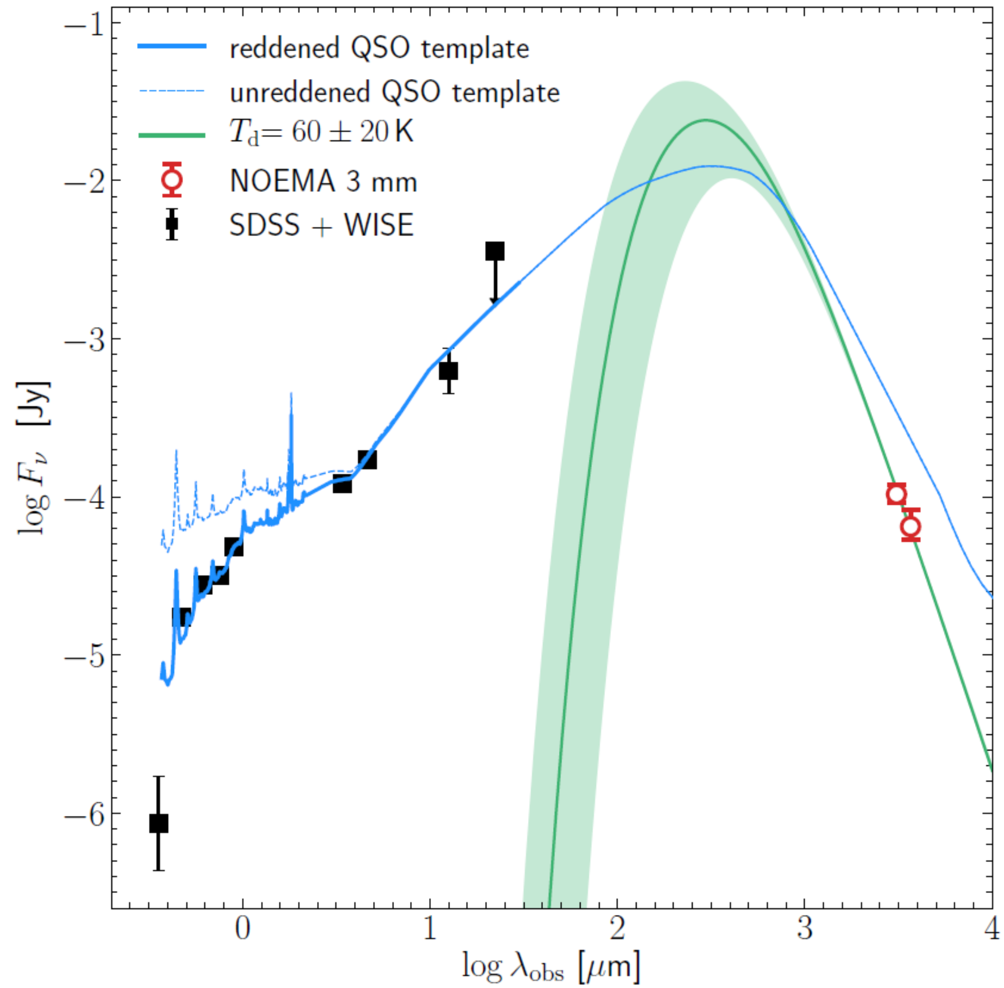

⇒

$$\log L_{IR}/L_\odot = 12.2 - 13.1$$

$$\log L_{bol}/L_\odot \approx 13.4$$

J0015+1842. NOEMA observations

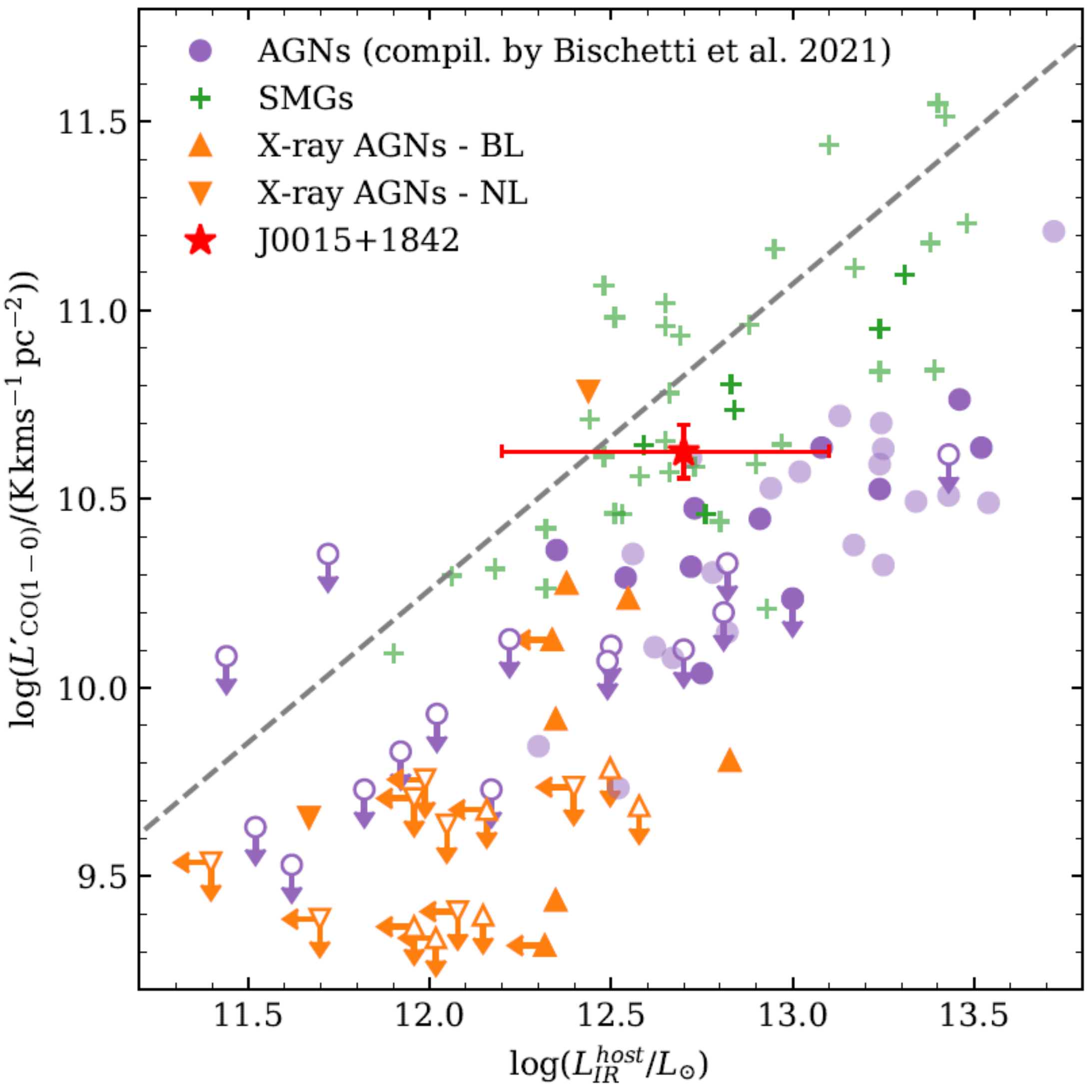

$$\log L_{IR}/L_\odot = 12.2 - 13.1$$

$$\log L_{bol}/L_\odot \approx 13.4$$

$\Rightarrow$

But J0015+1842 is a "regular" type I QSO:

$$A_V \sim 0.3$$

$$M_{BH} \approx 10^{8.6-8.9}\, M_\odot$$

$$\frac{L_{bol}}{L_{Edd}} \gtrsim 1$$

J0015+1842. NOEMA observations

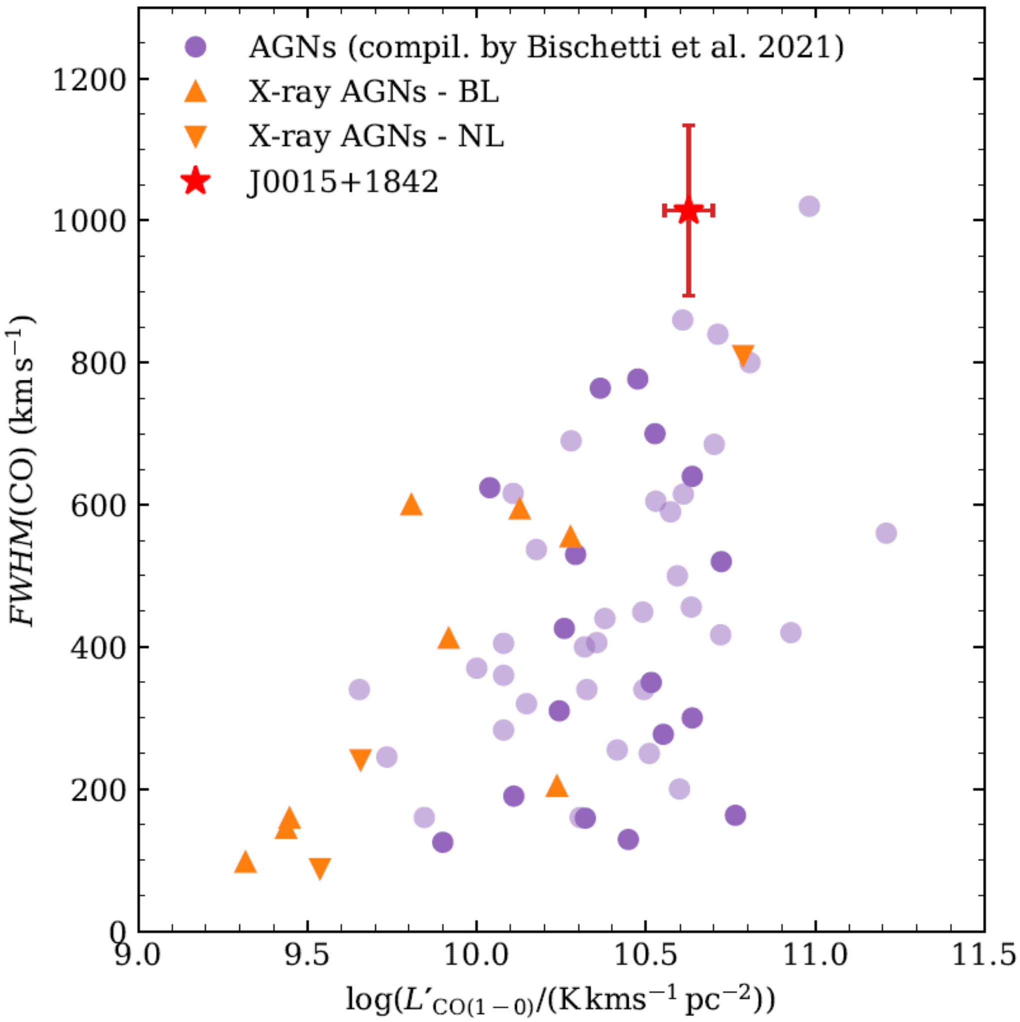

$$FWHM =$$
$$= 1010 \pm 120 \text{ km s}^{-1}$$

$\Downarrow$

Merger?

J0015+1842. General picture

X-shooter + NOEMA observations suggest that

1. J0015+1842 is a stage where a massive merger has brought significant amounts of gas towards an AGN.

2. The quasar has already cleared the way towards the observer, through powerful outflows.

⇓

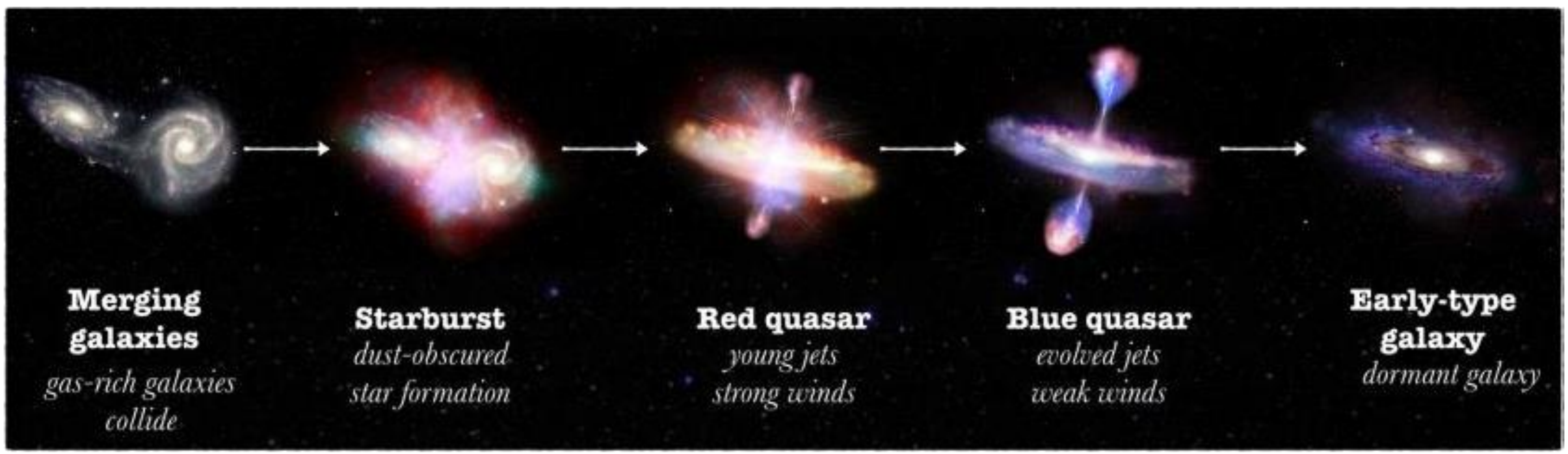

Summary

1. Proximate H_2-bearing DLAs with Lya leakage is likely very efficient way to preselect QSO outflows at high z.

2. Population of H_2 rotational levels allow to constrain physical conditions in outflowing gas (and hence the distance to central engine).

3. Follow-up observations of the first object J0015+1842 indicate:

X-shooter (optical)

   i. Extended emission in [OIII], CIV and Lya → outflow.

   ii. H_2 located at ~10 kpc distance from AGN

NOEMA (3 mm)

   iii. A large M_{mol} with large velocity dispersion → merger?

   iv. QSO is already cleared the way by outflow + orientation

Millimetron (>0.07 mm)

4. Probably bright future with Millimetron (H_2 and CO emission in outflow, properties of the host at mm and sub-mm)?